TECHNO-ECONOMIC ASSESSMENT OF PSO OPTIMIZED MICROGRID WITH HYDROGEN STORAGE SYSTEM

by

ARAFAT IBNE IKRAM

MD. KAMRUZZAMAN ROCKY

BACHELOR OF SCIENCE IN ELECTRICAL AND ELECTRONIC ENGINEERING

Department of Electrical and Electronic Engineering
INTERNATIONAL ISLAMIC UNIVERSITY CHITTAGONG

JULY 2022

TECHNO-ECONOMIC ASSESSMENT OF PSO OPTIMIZED MICROGRID WITH HYDROGEN STORAGE SYSTEM

by

ARAFAT IBNE IKRAM

MD. KAMRUZZAMAN ROCKY

A thesis
submitted as partial fulfilment of the requirement for the degree of

BACHELOR OF SCIENCE IN ELECTRICAL AND ELECTRONIC ENGINEERING

Department of Electrical and Electronic Engineering
INTERNATIONAL ISLAMIC UNIVERSITY CHITTAGONG

JULY 2022

CERTIFICATE OF APPROVAL

The thesis/project entitled as **" Techno-Economic Assessment of PSO Optimized Microgrid with Hydrogen Storage System"** submitted by **Arafat Ibne Ikram**, bearing Matric ID. **ET173001** and **Md. Kamruzzaman Rocky**, bearing Matric ID. **ET173017** of session **Spring 2021**, to the Department of Electrical and Electronic Engineering, International Islamic University Chittagong, has been accepted as satisfactory in partial fulfilment of the requirements for the degree of Bachelor of Science in Engineering and approved for the examination held on **22 JULY, 2022**.

_____

Supervisor
Engr. Md. Rashidul Islam
Assistant Professor
Department of Electrical and Electronic Engineering
International Islamic University Chittagong

DECLARATION

It is hereby declared that this work has been done by us and no portion of the work contained in this thesis/project has been submitted elsewhere for the award of any degree or diploma.

_____

Arafat Ibne Ikram

_____

Md. Kamruzzaman Rocky

ACKNOWLEDGMENT

All praises and thanks to Allah, the Lord of the world, the Most Beneficent, the Most Merciful, to complete this thesis without Whose help it would not be possible for us.

We appreciate our gratitude to our honorable thesis supervisor **Engr. Md. Rashidul Islam**, Assistant Professor, Department of Electrical & Electronic Engineering, International Islamic University Chittagong for his useful ideas and assistance for the thesis work. He has given us guidelines to correct our work.

We are also grateful for the kind support of faculty members of the Department of EEE.

We owe to all those authors and researchers whose work we used in the creation and development of this study.

Finally, We want to thank our parents very heartily for their encouragement and their inspirations, who are the continuous source of motivation to carry out this four-year journey and specially this research.

Authors

ABSTRACT

Microgrids are designed to utilize the renewable energy sources and it is a revolutionary choice in terms of reducing the environmental effect of excessive GHG emissions while producing electricity. The intermittency of renewable generation poses challenges to the technical and economic feasibility of microgrid operation, which conveys the integration of hybrid energy storage systems. In recent decades, Several researched has already been concluded in search of reliable and economically feasible hybrid energy storage. Hydrogen storage have been considered to be a key vector for enhancing the effectiveness of renewable and sustainable energy storage. The hydrogen ecosystem would be deemed a fully green energy storage system if we could manufacture hydrogen from renewable energy sources, store it, and utilize it in times of energy shortage. Here we have presented a model for evaluating the technical, economical feasibility and the environmental impact on a Grid-connected Microgrid integration scenarios consisting hybrid energy storage system. Microgrid model was comprised Photovoltaic Panel, Wind turbine, Lead-Acid battery, Electrolyzer, Fuel cell, and $H2$ cylinder tank. Microgrid component's analogous model was presented by the mathematical function by which we estimated annual hourly renewable generation based on given resources. In order to consider the load uncertainty, load consumption model for 50 homes was generated using Gaussian process. The microgird components sizing was done by Particle Swarm optimization technique (PSO) to minimize the installation upfront cost as well as levelized cost of energy ($/kWh). We used an energy dispatched strategy for smartly distribute energy among energy storage's and load consumption model and reduce the loss of power supply probability (LPSP). We tested different microgrid's energy penetration levels of 25%, 50%, 75% and 100% in terms of peak power distribution capabilities to load demand respective to conventional grid, where, Microgrid's 100% integration capabilities try to maintain the full load demand and not bought energy from conventional grid. And we found different LCOE and annual GHG emission for each integration scenario and easily distinguish which system performed better compared with other system.

TABLE OF CONTENTS

LIST OF TABLES

LIST OF FIGURES

LIST OF ABBREVIATIONS

MG	Microgrid
CG	Conventional Grid
IRR	Solar Radiation on Tilted Surface
SOC	State of Charge
CH	Charge rate of Battery
DCH	Discharge Rate of Battery
EDS	Energy Dispatch Strategy
PSO	Particle Swarm Optimization
EM	Electrolyzer Module
FC	Fuel Cell
AED	Annual Electricity Demand
MC	Maintenance Costs
RC	Replacement Costs
IC	Installation Costs
CRF	Capital Recovery Factor
TAC	Total Annual Cost
NPC	Net Preset Cost
LCA	Life Cycle Assessment
LCOE	Levelized Cost of Energy

CHAPTER 1
INTRODUCTION

1.1 Introduction

Global warming has been regarded as one of the most massive environmental concerns that have captivated the world's attention in recent decades. Industrialization and urbanization in many developing nations have contributed to the increase in carbon emissions in the atmosphere, which has resulted in an increase in Greenhouse gas levels [1]. Many regions of the world are suffering drought and are no longer suited for commercial agriculture, because of less rain, and sudden temperature increase. Land use and management have been shown to have a bigger influence on soil conditions than climate change's indirect effects, yet adaptive behavior has the ability to mitigate these effects. Even if all carbon dioxide levels stopped immediately, climate conditions would continue to evolve [2]. The present amount of pollution caused by humans and the random release of greenhouse gases into the air could make global warming, rising sea levels, desertification, and weather changes worse. Global energy production, development, and consumption are in a continual state of transition, with the rise and implementation of new renewable technologies in emerging nations serving as proof [3]. A study shows the Sun emits four million exa-joules (1 EJ = 1018J) of energy every year, and which can easily be harnessed using Solar Photo-Voltaic Panel and Concentrated Solar Power plant [4]. Empirically Solar energy has the potential to fulfill the world's energy demands, if technology is correctly deployed [5]. Another key aspect regarding solar energy is, Global carbon emissions have emerged recently as a serious global environmental, social, and economic concern that can also be mitigated by utilizing solar energy [6].

In recent years, environmental deterioration has become a widespread problem in many developing nations due to the excessive emission of carbon dioxide and other greenhouse gas in the atmosphere [7]. Electricity generation relies heavily on fossil fuels, which are one of the major source of greenhouse gas emission worldwide. In US about 0.386 kg of CO_2 equivalent gas release on kilowatt/hour of electrical energy production [8]. It is anticipated that the high CO_2 concentration in the atmosphere would continue to rise, if the issue of CO_2 emissions is not addressed. In 2019, it was estimated that the average Concentration of carbon dioxide in the atmosphere ($414,7\ ppm$) was 45% higher than

between 1980 and 1990 [9]. Utilizing the Renewable energy is currently the best counter step to minimize the GHG emission and evidently fight climate change.
According to IRENA [10], Nearly 60.07% of the world's most recent grid-connected PV systems were installed in China, with the United States coming in second with about 11.9% percent [11]. Considering annual solar radiation of 4.5 to 6.5 kWh/m^2, only 1,800 MW of Solar photovoltaic panels are installed in South Africa [12].

1.2 Motivation

The demand of renewable generation continues to rise because of the environmental concerns. Consequently, the upfront cost of microgrid is huge. The optimal design of a renewable energy system may substantially enhance the economic and technical performance of the power supply. Therefore, minimizing the number of components required for microgrid will reduce the high initial investment and energy costs. We have proposed a grid-integrated microgrid model and **Optimize the Tehcno-Economical Parameter Using PSO and Evaluate the Environmental Performance of The System** in different penetration level scenario considering load intermittency.

1.3 Objective of this Thesis

Due to the unpredictability and uncertainty of renewable generation in hybrid renewable systems, a dispatchable energy source such as conventional grid is incorporated to increase system stability. The key goals of this thesis are as follows:

1. To design a grid-connected microgrid system that comprise with primary generation unit such as Solar PV panels and Wind turbine and energy storage system using mathematical mode that can sell electrical energy to the conventional grid in the time of excess generation and purchase energy from conventional grid in the time of energy shortage.

2. To optimize the number of components needed for economically feasible renewable plant using Particle Swarm Optimization technique, which will reduce the installation cost and the levelized cost of energy considering various MG-CG integration scenario.

3. To reduce the annual greenhouse gas emission and the Environmental impact of considering various MG-CG integration scenario.

In this thesis, We described our thesis work in 5 chapter where the thesis outline are described as follows:

Chapter 1 : This chapter contains the Introduction and background works of thesis work. In this chapter, we discussed the various problem regarding traditional conventional grid, and why it is important to seek alternative sustainable renewable energy. and also consider hybrid energy storage system.

Chapter 2 : This chapter contains the Literature review of previous works. In this chapter we discussed about all related previous works related to this thesis works.

Chapter 3 : This chapter contains the methodology where the we developed every component such as technical and economical model used in this thesis works using mathematical equation.

Chapter 4 : This chapter contains the implementation of result where the result and implementation of our thesis and Cost analysis where the per unit price of this project has been discussed.

Chapter 5 : This chapter contains the Conclusion and future scope where conclusion and future possible field of the thesis has been discussed.

CHAPTER 2

Literature Review

2.1 Introduction

In this chapter, We have provided a comprehensive overview of the thesis study and associated literature. Afterwards, we included some fundamental description and necessary components of microgrids and and optimization technique which was implemented on the microgrid model. Later we shortly brief about why it is necessary to optimize microgrid parameter and the impact of microgrid on power system.

2.2 Summary of Previous Work and Research Gap

In hybrid Renewable systems, size optimization and energy management are two most essential considerations. Renewable generation is uncertain and cost is very high compared with conventional grid electricity generation. However, Worlds have taken initiative in the green electricity generation due to severely reason. So it is important for microgrid to have an optimal configuration and which is economically feasible. Several approach have been taken throughout the year for microgrid to have a excellent up time with reasonable upfront cost. So it is necessary to optimize microgrid sizing and energy management for reducing the upfront cost, and cost of energy for a green energy generation.

2.2.1 Previous Works

The environment and human health have been found to be negatively impacted by CO2, a greenhouse gas pollutant.Therefore, there is an urgent need to reduce CO2 emissions, and with relation to electricity generation, this may be achieved by using renewable energy sources with low carbon footprints like solar photovoltaics (PV) and wind turbines [4]. One of the biggest problems with renewable energy sources, despite their environmentally friendly methods of production, is the weather-related intermittency of their supply [13]. This mismatch has been addressed by a number of ways. When it comes to energy consumption, the demand may be changed to match the quantity of production [14]. Diverse sources, include solar power (PV), wind energy (WT), diesel generators (DG), fuel cells (FC), etc. which are complementary to one another might be used to reduce the mismatch [15]. Utilizing energy storage devices, such as batteries, capacitors, etc., is another suggestion for a solution. During times of peak demand for electricity [16]. The

energy generation and storage options can be coupled in a MG, which is a system of related energy production, storage, and consumption devices that can operate individually or in conjunction with a conventional grid (CG) [17]. The MG must be sized properly to enhance dependability and cut costs. The MG must be sized properly to enhance dependability and cut costs. There are assessments in the literature that have carried out these optimization studies based on the availability of renewable resources and regional power demand. Numerous studies have been conducted regarding size optimization and energy management in hybrid renewable systems, including energy storage modeling in the size issue [18], microgrid's component sizing and regulation potentiality [19], optimal sizing of energy storage in grid-connected mode [20], and multi-operation management in hybrid systems [21]. The optimal size of each component in a size optimization approach is calculated in relation to the given objectives. For the size optimization problem, many objectives can be set, such as cost and dependability, for a size optimization challenge, many objectives such as cost and reliability might be stated. Hybrid system size optimization has been tackled in two frameworks in the literature: single-objective and multi-objective. The majority of research has focused on size optimization as a single-objective issue.

2.2.2 Research gap

As a result of our research, we believe it is necessary to investigate the efficacy of Hybrid energy storage system in grid connected microgrid scenario. Hybrid energy storage management is comprises with both hydrogen storage and traditional battery storage system. Even though Hydrogen storage system is extremely expensive and low in efficiency, it is claimed be the most environment and climate compatible (causing the least damage), energy storage medium [22], [23]. Here, we set up a grid-integrated microgrid scenerio which have hybrid energy storage system. Firs we optimized size parameter. later we evaluates cost of energy, environmental impacts (LCA) of a MG over its entire life cycle.

2.3 Microgrid

Microgrid is viewed as a group of Renewable Energy Sources (RES's) such as solar panels, wind-turbines, and Energy Storage Systems (ESS) in combination to Electrical Loads that run locally as a single controlled entity. A microgrid operates at a low voltage and able to provide electricity to a home, workplace, university, hospital, and so on. A MG system can work simultaneously both with or without being connected to the

main power grid. A Stand-alone MG are better suited to service local energy sources if electricity transmission and distribution from a big centralized source is too remote and costly to carry out. In rural parts of the country, micro-grid is the most effective method for consuming electricity; thus, it supplies power in an emergency and someone relies on this micro power system entirely [24] . Low or medium voltage distribution systems perform successfully and efficiently when they are part of an integrated MG system, which implies that they have a common operating strategy and control approach.

2.3.1 Optimizations of Microgrid

Grid-connected Micro-grids faces many challenges while operating. Reducing the operation Costs is the first obstacle. Meanwhile, the intermittent nature of renewable energy sources like solar photovoltaic (PV) and wind-turbine (WT) due to changes in the weather, which can cause issue with power balance and power quality. The first step is to choose the optimal link to the physical model components, which encompass Renewable Energy Sources, Energy Storage Systems, electrical loads consumption model, and power converters that connect all system components [25]. The energy management system (EMS) plays a crucial role in minimizing the running cost of MG by managing the production and/or flow of electricity. The EMS regulates the power flow in the MG based on optimum cost and gives reference values to the MG's local controller. The concept of energy management in order to supply baseline data to control centers has previously been analyzed. A optimization needs to carry-out in-order to find a stable and economic solution. To mitigate the cost minimization dilemma, several optimization techniques have been developed over decades. MG optimization mainly focus on cost minimization considering the intermittency of renewable generation and first priority is fulfilling the load demand.

2.3.2 Types of Microgrids

Grid-connected microgrid: Grid-Connected micro-grid is interconnected with a point of common coupling (PCC) and is being operated in parallel with existing conventional grid. It facilitate the conventional grid with potential capacity, power quality and reliability, and voltage issues by providing with synchronized frequency and voltage to facilitate.

Stand-alone microgrid: A stand-alone micro grid system can be developed by utilizing most of renewable energy by hybrid energy storage systems to sustain the intermittent and infrequent renewable energy resources. On stand-alone micro grid environment diesel

generator serves as a secondary or backup sources of energy in case of extreme weather condition which may fail the renewable generation [26]

Networked microgrid: Networked Microgrid is a nested Hybrid systems that comprise of several renewable energy sources (RESs) and distributed energy resources (DERs) which are interconnected to the same conventional grid circuit sector and serves electrical energy to a a large geographical region. An oversight control system handles and improves networked microgrids to run and synchronize each grid-connected or island mode at different levels of the hierarchy along a conventional grid [27]

2.3.3 Microgrids Essential Components

Renewable Energy Sources: Renewable Energy Sources are regarded as clean energy sources, and effective usage of these resources minimizes environmental consequences, produces little residual waste, and is sustainable given current and future economic and social communal demands. The primary sources of energy is sun. Solar energy is transmitted to earth and absorbed by the environment in a variety of ways. Most of the solar energy can be harnessed by concentrated solar plant and Solar photovoltaic panel. Some solar energy is composed the movement of air relative to Earth's surface which is known as wind energy.

Energy Storage System: The Energy Storage System is regarded as a valuable device for increasing reliability and flexibility, because renewable generation rate is very uncertain and weather dependent. Energy storage system is designed in such way that can maintain the load demand in the time of no generation.

Point of Common Coupling: In grid-connected microgrid scenario, Point of Common Coupling (PCC) is junction point between microgrid and conventional grid. PCC is a central point of connection for multiple consumers that are connected to the same utility power source [28]. In remote locations standalone microgrids where joining to the main grid is not feasible either to technological or economical restrictions that are regarded as Non-PCC.

2.3.3.1 Solar PV Panel

Solar Photovoltaic panel (PV) is a renewable energy generator which harness the solar energy and convert them into electrical energy. solar cell is the fundamental component of a solar Module which is basically a p-n junction assembled in a thin semiconductor substrate or layer. The photovoltaic effect can directly convert solar energy's electromag-

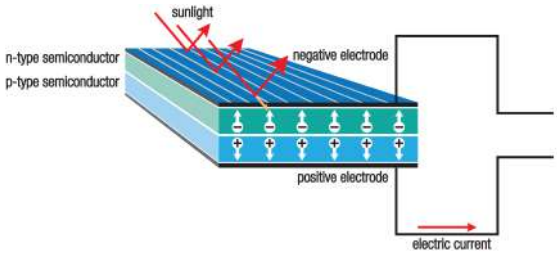

Fig. 2.1 Internal Diagram of Solar PV Panel and Modules [30]

netic radiation into electricity. When light enters to a solar cell, photons with an energy higher than the semiconductor's band-gap energy are absorbed, leading to the formation of electron-hole pairs proportional to the incident irradiation. These carriers are carried off from the p-n junction's internal electric fields, producing in a photo-current that is directly proportional to solar radiation [29]. Solar Panel is made of solar modules and the module is made of solar cells. Electrical connections between solar cells in series and/or parallel circuits enabling cells to produce higher voltages, currents, and power levels. PV panel and modules internal diagram is showing in **Fig. 2.1**.

2.3.3.2 Wind Turbine

Wind turbine is like an alternator, Which basically works when the aerodynamic force of air hits the rotating blade of turbine, and the moving blade turns the rotor of alternator. This process converts wind energy to mechanical energy, and converts the mechanical energy into electrical energy. In renewable energy systems, the different types of renewable energy are converted to electrical energy using static systems or by rotating generators. Solar Photovoltaic panel and Wind turbine are both considered as to be one of the primary source renewable energy generation. The internal diagram of Wind turbine was shown in **Fig. 2.2**.

2.3.3.3 Hydrogen Energy Storage

Hydrogen energy storage is unique in that it provides a general-purpose mechanism of storing energy that may later be employed in a variety of applications. The gas is appealing since it is a low-carbon energy source because it does not emit carbon dioxide while usage (although it does emit carbon dioxide during manufacturing). As a result, hydrogen energy storage might be one of the most essential energy storage options accessible.

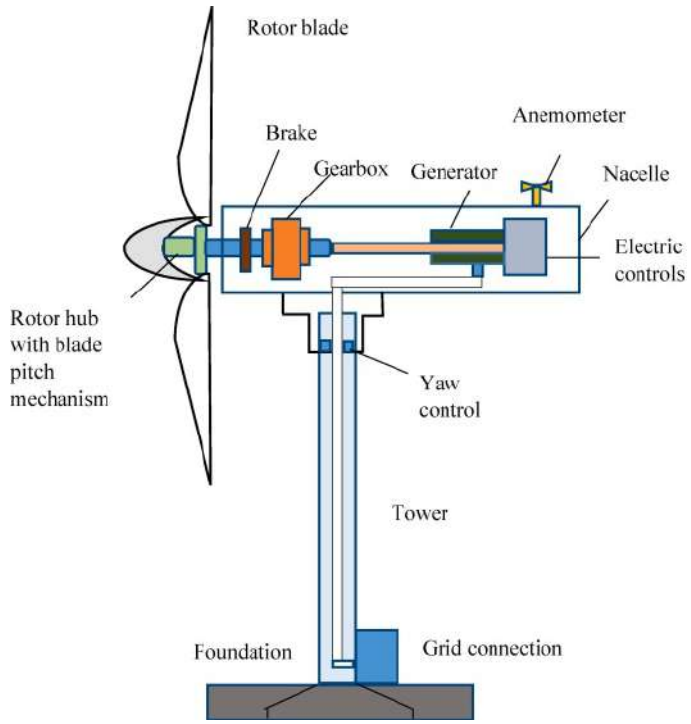

Fig. 2.2 Internal Diagram of Wind Turbine [31]

2.3.3.4 The Principles of Hydrogen Energy Storage

Hydrogen energy storage is another form of chemical energy storage in which electrical power is converted into hydrogen. This energy can then be released again by using the gas as fuel in a combustion engine or a fuel cell. Hydrogen can be produced from electricity by the electrolysis of water, a simple process that can be carried out with relatively high efficiency provided cheap power is available. The hydrogen must then be stored, potentially in underground caverns for large-scale energy storage, although steel containers can be used for smaller scale storage.

2.3.3.5 Electrolyzer

In the process of electrolysis, an electrolyzer utilizes electricity to split water into hydrogen and oxygen. The electrolyzer system generates hydrogen gas by electrolysis. The remaining oxygen is either discharged into the environment or caught and stored to serve other industrial operations or, in certain situations, medicinal gases. Electrolyzers can range in size from tiny, appliance-sized equipment that is well-suited for small-scale dispersed hydrogen production to large-scale, central production facilities that might be directly linked to renewable or other non-greenhouse-gas-emitting types of power generation. **Fig. 2.4** shows the internal core diagram of Electrolyzer Module.

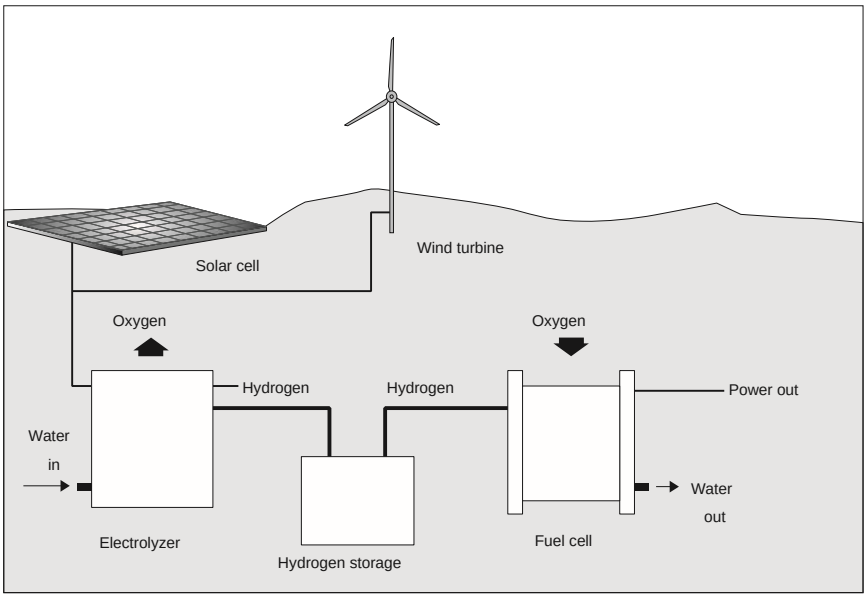

Fig. 2.3 Simple hydrogen energy storage system [32]

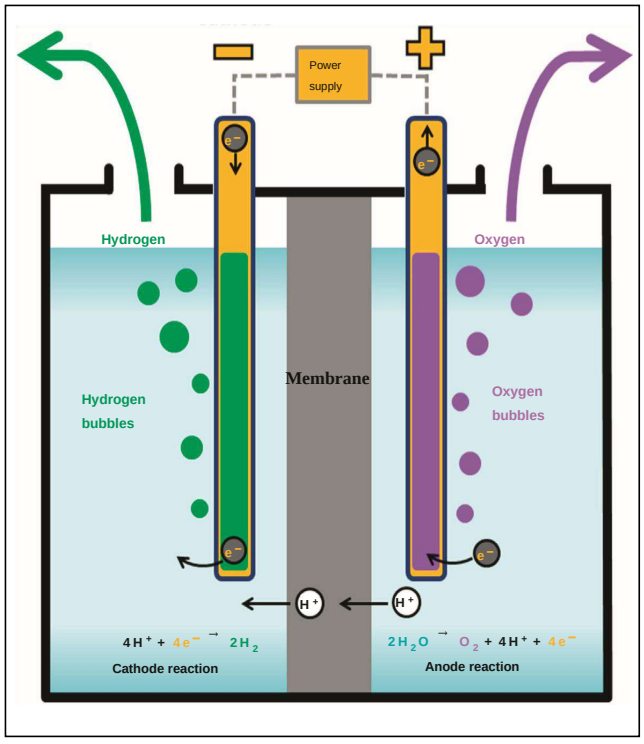

Fig. 2.4 Internal Diagram of Electrolyzer Core [33]

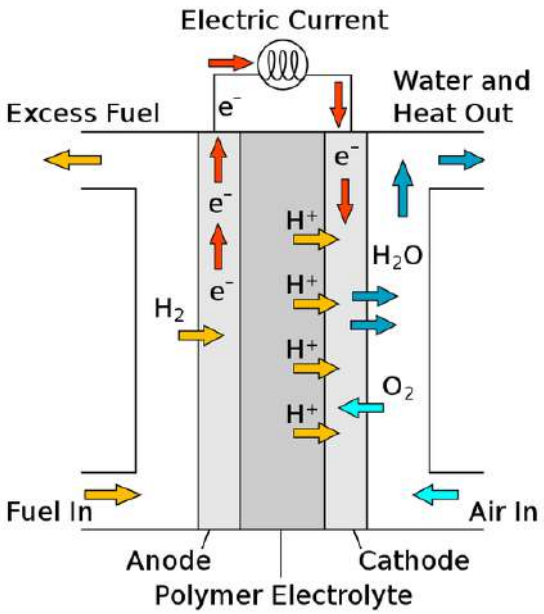

Fig. 2.5 Internal Diagram of Fuel Cell Core [34]

2.3.3.6 Fuel Cell

A fuel cell produces electricity using the chemical energy of hydrogen or other fuels in a clean and efficient manner. Only electricity, water, and heat are produced when hydrogen is used as a fuel. Fuel cells are one of a kind in terms of the wide range of applications they may be used for.They may run on a variety of fuels and feedstocks, and they can power systems as large as a utility power plant or as tiny as a laptop computer. Internal diagram of Fuel cell is similer to Electrolyzer core, **Fig. 2.5** shows the internal core diagram of PEM Fuel Cell.

2.3.4 Impacts of micro-grid on power system

A micro-grid is able to operate in Grid-connected and stand-alone modes and handle the transition between the two. In grid-connected mode, auxiliary services may be offered by exchanging energy between the microgrid and the main grid.There are many other possible income sources [35]. In the lack of renewable energy sources, microgrids provide a way to reconcile the requirement for carbon-reduction while simultaneously offering reliable power over time. Microgrids are also safeguarded against adverse weather conditions and natural catastrophes since they lack massive assets or miles of over-the-air cables and other electric infrastructure that must be maintained or restored after such occurrences. Microgrids and the incorporation of DER units in general present some operational challenges in the design of control and security devices to ensure that the

current level of reliability is not significantly impacted, and that the potential benefits of distributed generation (DG) devices are fully exploited [35], [36]. Some of these difficulties are the result of ideas that were formerly applicable to conventional distribution networks but are no longer relevant, while others are the result of transmission system-level dependability concerns. The inclusion of DGs in a low-voltage network may result in reverse power flows, which can lead to safety synchronization issues, undesired power flow patterns, and defective current and voltage controllers. Interactions between the DG unit's control system might result in local oscillations, necessitating a thorough study for stabilizing small disturbances. Moreover, transitional activities between networks and isolated operating modes in a microgrid (standalone) might cause momentary instability. In recent years, research has shown that the microgrid interface of direct current (DC) would result in an enhanced management system, more energy-efficient distribution, and higher current capability for the same ratings [37]. Microgrids differ from bulk power networks in their low inertia, which enables a relatively high number of synchronous generators. This effect is notably evident in microgrids with a high proportion of DG interactive power units. In the absence of an appropriate control mechanism, low system inertia may result in large frequency variations during Island mode operation. Synchronous generators run at the same frequency as the grid, dampening rapid frequency shifts. Syn-chronverters imitate the frequency control of synchronous generators. [37], [38]. The regulation of the battery energy storage or the flywheel for frequency balancing are other option.

2.3.5 Particle Swarm Optimization

Particle swarm optimization is a novel evolutionary computing approach that was just designed and introduced [39]. This method blends evolutionary calculations with social psychology concepts in socio-cognition human agents. The behavior of species such as fish schooling and bird flocking inspired PSO. In general, PSO is described as having a basic principle, being straightforward to implement, and being computationally efficient [40]. PSO, unlike other heuristic algorithms, provides a flexible and well-balanced mechanism for improving global and local exploration capabilities.

- The PSO approach, like evolutionary algorithms, performs search utilizing a population of particles that correspond to persons.

- Each particle represents a potential solution to the current challenge.
- Particles in a PSO system change locations by flying around in a multi-dimensional search space until they reach a somewhat stable position, or until computational restrictions are reached [41].
- A social-only model and a cognition-only model are combined in the PSO system. Individuals overlook their personal experiences and alter their conduct based on the neighborhood's successful ideas, according to the social-only component. Individuals are treated as solitary creatures in the cognition-only component. These models allow a particle to modify its location.

2.3.6 Advantages Particle Swarm Optimization

The following are some of the advantages of PSO over other classic optimization techniques:

- PSO is a population-based search method, which means it has parallelism built in. PSO is less likely to become stranded on local minima as a result of this characteristic.
- PSO employs performance index or objective function information to direct the search in the issue space. As a result, nondifferentiable objective functions are no problem for PSO. This trait also frees PSO from the assumptions and approximations that older optimization methods typically demand.
- PSO employs probabilistic rather than deterministic transition rules. As a result, PSO is a stochastic optimization method capable of searching a complex and uncertain area. As a result, PSO is more adaptable and durable than traditional approaches.

CHAPTER 3

METHODOLOGY

3.1 Introduction

This chapter addresses how we used mathematical formulas to establish a model of a Grid-Connected Hybrid Renewable System in MATLAB. Additionally, we went into great depth about the mathematical analogous interpretation of our hybrid system, estimated the annual hourly output energy and economical analysis of our model.

3.2 Methodology

The methodology for microgrid system diagram was shown in "**Fig. 3.1**" where we went through the underlying function and mathematical interpretation of each component of MG.

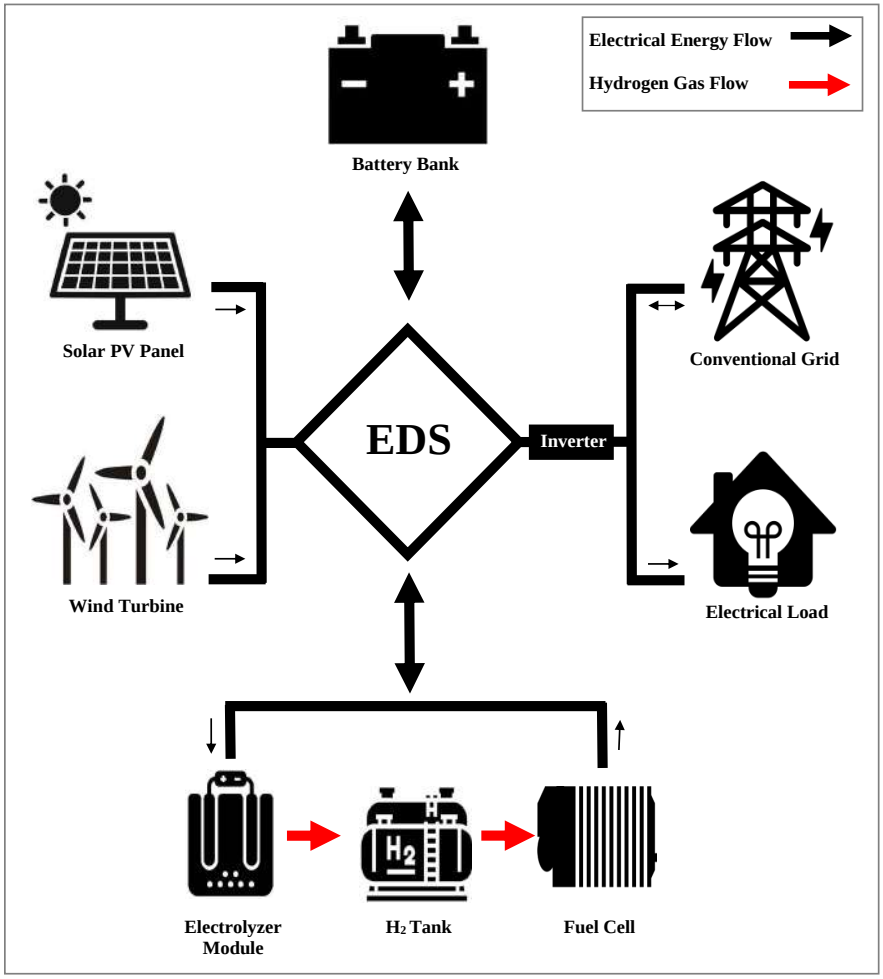

Fig. 3.1 System Schematic Diagram

We implemented an Energy Dispatched Strategy and minimized the **LCOE** and **GHG emission** using optimization technique. Here, in **Fig. 3.1**, Both PV and WT were used as primary renewable generator. Microgrid System was connected with load, grid other energy storage system. Hydrogen Storage system was connected with Electrolyzer and Fuel cell. When the generation is higher, excess energy can be used to fill up the energy storage, and when the energy is deficit, the shortage energy could be bought from conventional grid

3.3 Solar Modeling and Concept

Solar Photovoltaic generator simulation consists of two key parts: Solar Irradiance on a Titled Surface Plane and the Photovoltaic Module Model.

3.3.1 Solar Irradiance on a Titled Surface

The best performance from a solar photovoltaic module achieved by tilting it at certain angle and the location where the system will be installed determines the orientation and the tilt of the solar panels. So in order to simulate the solar radiation on tilted panel, We must know the main component of solar irradiance. These three main components of solar irradiance are direct, sky-diffuse, and ground reflected was shown in **Fig. 3.2** .

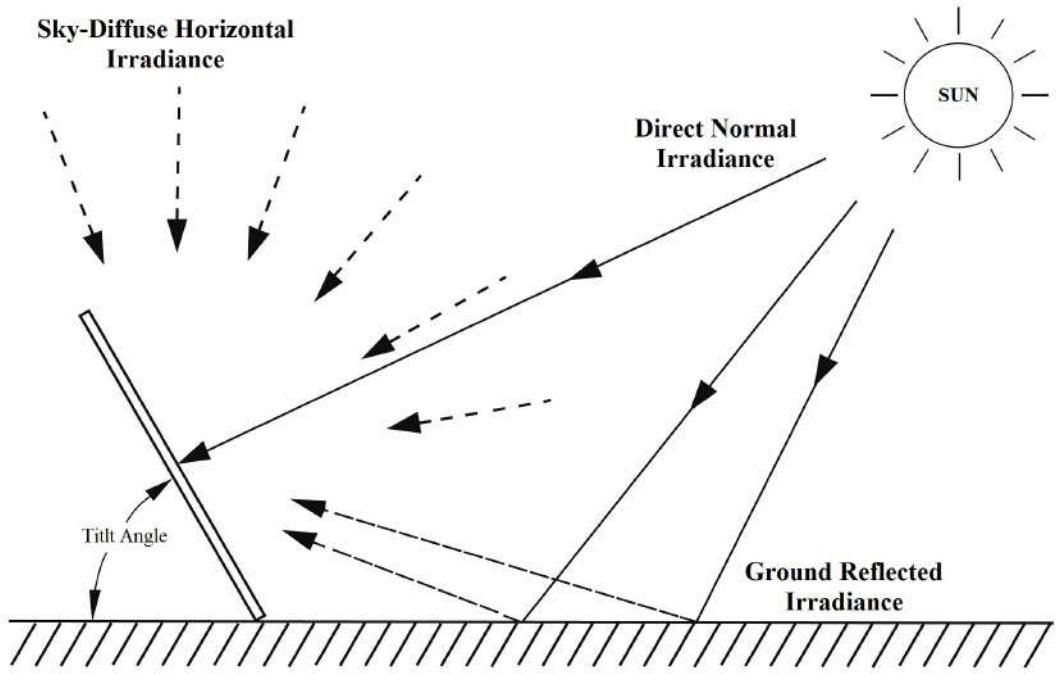

Fig. 3.2 Components of Solar Irradiance [42]

In order to simulate, the hourly solar irradiation ($IRR\ W/m^2$) on a tilted photovoltaic

panel - we used the equation (3.1) [43]. The solar DNI, DHI and Clearness Index data was collected from NASA [6].

$$IRR(t) = IRR_{direct}(t) + IRR_{diffuse}(t) + IRR_{reflected}(t) \tag{3.1}$$

Direct parts of solar irradiance (IRR_{direct}) **:** we used (3.2) to estimate the direct components of solar irradiance [43].

$$IRR_{direct}(t) = DNI(t) - DHI(t)\left(\frac{cos\theta}{cos\theta_z}\right) \tag{3.2}$$

Where, $\theta = 40°$, and $\theta_z = 38°$ was solar incidence angle, and the zenith angle respectively.
Sky-Diffuse parts of solar irradiance ($IRR_{diffuse}$)**:** We used the equation (3.3) to correlate the effect of cloudy condition with the diffuse horizontal irradiance component (DHI) to measured the Sky-Diffuse component of solar irradiance [44].

$$IRR_{diffuse}(t) = DHI(t)(0.5(1 + cos\frac{\beta}{2}))(1 + f_k(t)(sin\frac{\beta}{2})^3)(1 + f_k(t)(cos\theta))^2 sin(\theta_z)^3) \tag{3.3}$$

$$f_k(t) = 1 - \frac{DHI(t)}{DNI(t)} \tag{3.4}$$

Where, $f_k(t)$ was the hourly cloudy condition [44]..
Ground-reflected parts of solar irradiance ($IRR_{reflected}$) **:** We calculated the ground-reflected components of solar irradiance using the equation (3.5).

$$IRR_{reflected}(t) = \frac{\rho}{2} GHI(1 - cos\beta) \tag{3.5}$$

Where, $\beta = 20°$ was the Solar Panel Tilt Angle and $\rho = 0.2$ was the albedo which measure of the diffuse reflection of solar radiation out of the total solar radiation.

3.3.2 Solar Photovoltaic Panel Model

The solar photovoltaic cell is basically a p-n junction semiconductor, whose photo-current is directly proportional to solar radiation [29]. The total generated power by

Table 3.1 PV Module Specified Data [48]

Name	Symbol	Value
Rated Power	P_{pv}	$435W$
Cell Efficiency	η	22.5%
Rated Voltage	V_{mpp}	$72.9V$
Rated Current	I_{mpp}	$5.97A$
Open-circuit Voltage	V_{oc}	$85.6V$
Short-circuit Current	I_{Sc}	$6.43A$
Wind velocity of cell	v	$2m/s$
Reference Temperature	T_{ref}	$25°C$
Ideal Factor of cell	A	1.3
Number of modules in series	Nm_S	10
Number of modules in parallel	Nm_p	2
Number of cells in series	N_S	128
Number of cell in parallel	N_p	1

photovoltaic panel can be obtained by using the equation (3.6) [45].

$$P_{pv} = V_{max} \times I_{max} = \gamma V_{oc} I_{sc} \tag{3.6}$$

Where, the values open-circuit voltage V_{oc}, short-circuit current, I_{sc}, terminal voltage (V_{max}), and fill factor (γ) were given on Table 3.1. Output current (I_{max}) was calculated using equation 3.7. We used the equation (3.7) in order to estimate the output current from one solar panel [45]–[47]. All the parameter value were given on **Table 3.1** .

$$I_{max} = N_p I_{ph} - N_p I_s \times \left[\exp\Big(q\Big(\frac{v}{N_s k T_c A}\Big) - 1\Big)\right] \tag{3.7}$$

We calculated the light-generated current or photo-current (I_{ph}), and the saturation current (I_S) (3.8), and (3.9) respectively [45]–[47].

$$I_{ph} = [I_{sc} + K_1(T_c - T_{ref})]\lambda \tag{3.8}$$

$$I_s = I_{rs} \times (\frac{T_c}{T_{ref}})^3 \times \exp\left[\frac{qE_g\Big(\frac{1}{T_{ref}} - 1\Big)}{kA}\right] \tag{3.9}$$

Here, Solar irradiation λ was obtained from equation (3.1). $E_g = 1.11eV$, was the Band-gap Energy of Semiconductor, $q = 1.6 \times 10^{-19}C$ was charge of one electron, and $k = 1.38 \times 10^{-23}J/K$ was the Boltzmann's constant.

3.4 Wind Turbine Model

We used the quadratic model of wind turbine. Equation (3.10) to calculate the output power of Wind Turbine.

$$P_{WT}(t) = \begin{cases} WT_{rate}\left(\frac{V - V_{in}}{V_{rate} - v_{in}}\right) \text{ for } v_{in} \leq V \leq v_{rate} \\ WT_{rate} \text{ for } V_{rate} < V < V_{out} \\ 0 \text{ for } V < V_{in} \text{ and } V > v_{out} \end{cases} \tag{3.10}$$

Where, WT_{rate} was the rated power of wind turbine, $V(m/s)$ was the wind velocity, $V_{rate}(m/s)$ was the rated wind velocity, $V_{in}(m/s)$ was the cut-in wind velocity, and $V_{out}(m/s)$ is the cut-of wind velocity. The respective data of these parameter were given on Table 3.2.

Table 3.2 Wind Turbine Specified Data [49]

Name	Value
Rated Power of wind turbine, (WT_{rate})	$1000W$
Rated Wind Velocity (V_{rate})	$12\ m/s$
Cut-in Wind Velocity (V_{in})	$3\ m/s$
Cut-off Wind Velocity (V_{out})	$23\ m/s$

3.5 Energy Storage System Modeling

We estimated the the amount of energy accessible in a energy storage at a given moment using the following equation (3.11) [50].

$$SOC(t) = SOC(t-1) + \frac{\eta_{ch}(t).CH.\Delta t}{BatteryCapacity} + \frac{DCH(t).\Delta(t)}{\eta_{dch}.BatteryCapacity} \tag{3.11}$$

Where, $BatteryCapacity$ was assumed to be $1000aH$, $\eta_{ch} = 80\%$ was the battery charging efficiency, $\eta_{dch} = 95\%$ was the battery discharging efficiency, and t was the hourly representation.

Hourly charging and discharging rate of battery was calculated using equation (3.12) and (3.13).

$$CH = min\left\{(P_{Generation} - P_{Load})\left[\frac{(SOC_{max} - SOC(t)).BatteryCapacity}{\eta_{ch}}\right]\right\} \tag{3.12}$$

$$DCH = min\{(P_{Load} - P_{Generation}).[(SOC(t) - SOC_{min}).\eta_{Dch}.BatteryCapacity]\} \quad (3.13)$$

$$SOC_{min} \leq SOC(t) \leq SOC_{max}$$

Here, $SOC_{min} = 20\%$ and $SOC_{max} = 80\%$ were the two main constrain of battery charging and discharging.

3.6 Electrolyzer Module Modeling

Water is split into hydrogen and oxygen by transferring electrons through the electrolyzer which is expressed by equation (3.14)

$$2H_2O + Electrical\ \ Energy \rightarrow 2H_2 + O_2 \quad (3.14)$$

We estimated the proportion of hydrogen produced and the total power consumed by a 1 kW rated power electrolyzer in 1 hour using the equation (3.15) and (3.16) [51].

$$\begin{aligned} H_2Produced &= \frac{I_{EM}N_{EM}}{2 \times F} \times \eta i \times 3600 \\ &= \frac{P_{EM}}{2 \times V_{EM} \times F} \times 3600 \end{aligned} \quad (3.15)$$

$$P_{EM} = I_{EM} \times V_{EM} \quad \eta i = 1 \quad (3.16)$$

Where, P_{em} was the Rated Power of the electrolyzer, $V_{EM} = 2V$ was the working voltage of electrolyzer.

Electrical efficiency of the electrolyzer ηe is the product of the current efficiency ηi and the voltage efficiency ηv, was shown in equation (3.17) [52].

$$\eta e = \eta i \times \eta v \quad (3.17)$$

The voltage efficiency ηv of the electrolyzer was assumed 47% and The current efficiency ηi of the electrolyzer was assumed 100% [51]

3.7 Hydrogen Compressor

H_2 gas produced by the electrolyzer needed to be compressed in order to stored on H_2 tank though adiabatic process. We included mathematical model for compressor in order to calculate the total electrical power consumed while compressing the Hydrogen and Storing it to the Cylinder. (3.18) was to used calculate the hourly energy consumed by hydrogen compressor [53], [54].

$$E_{compressor} = C_p \frac{T_1}{\eta_c} \left(\left(\frac{P_2}{P_1} \right)^{\frac{r-1}{r}} - 1 \right) m_c \tag{3.18}$$

Where, $\eta_c = 75\%$ is the efficiency of compressor, $C_p = 14304\ KJ\ (kg\ K)^-1$ is the specific heat of hydrogen at constant pressure, $T_1 = 293\ K$ is the gas temperature of Hydrogen, and $P_1 = 0.6MPa$ and $P_2 = 20MPa$ was inlet and output gas pressure of hydrogen tank, $r = 1.4$ was the isentropic exponent of H_2. For simulation purpose gas flow rate was assumed $(2.351\ s^-1)$.

From (3.15), $1kWh$ rated electrolyzer produced $9.33mol$ of Hydrogen gas and $0.0536kWh$ is consumed by Hydrogen compressor to compress $9.33mol$ of Hydrogen with pressure of $20MPa$ of compressed Hydrogen [53], [54].

3.8 Fuel Cell Modeling and Concept

Fuel cell works opposite of an Electrolyzer that converts the chemical energy of a fuel to electrical energy. The anode of a Fuel cell is periodically provided hydrogen gas, while the cathode Fuel cell is fed air (or pure oxygen). Equation (3.19) shows the chemical processes that occur at the anode and cathode.

$$2H_2 + O_2 \rightarrow 2H_2O + Electrical\ \ Energy \tag{3.19}$$

We estimated the total power generated and consumed by a 1 kW rated power Fuel cell in 1 hour using the equation (3.20) (3.21) [53], [55].

$$\begin{aligned} H_2Consumed &= \frac{I_{fc} N_{fc}}{2 \times F} \times \frac{1}{\mu_{fc}} \times 3600 \\ &= \frac{P_{fc}}{2 \times V_{fc} \times F} \times 3600 \end{aligned} \tag{3.20}$$

$$P_{fc} = I_{fc} \times V_{fc} \tag{3.21}$$

Where, P_{fc} was the rated power of fuel cells, μ_{fc} was Faraday's efficiency [54], $V_{EM} = 2V$ was the working voltage of fuel cell. and Fuel cell efficiency was assumed, $\eta_{fc} = 47\%$ [53].

3.9 Hydrogen Cylinder Modeling and Capacity Representation

Hourly Hydrogen generation was calculated using the equation (3.15). Hydrogen generated by EM was in Gas form. After using a compressor, the gas was compressed to liquid. Similarly Hourly Hydrogen consumption was calculated using the (3.20). Liquid Hydrogen was evaporate to Hydrogen Gas without any decompressor. Hydrogen generated by EM and Consumed by FC was presented in ($Molh^1$) unit. Then the Gas was compressed to liquid to fill the hydrogen tank. In order to convert ($Molh^1$) unit than in Energy analogous representation in (kWh) and, liquid volume represents in (Liter) for Hydrogen energy storage, we used equation (3.23), and (3.22) respectively [56].

$$V_{tank}(liter) = M_{tank} \times T_{tank} \times \frac{R}{P_{tank}} \tag{3.22}$$

$$E_{tank}(kWh) = M_{tank} \times 2 \times \frac{LHV(kWh\, kg^{-1})}{1000} \tag{3.23}$$

Where, $R = 0.08211\ atm\ (mol\ \ K)^{-1}$ was the gas constant, $LHV = 33\ kWh\ \ kg^{-1}$ is the low heat value of the hydrogen and Tank temperature $T_{tank} = 25°$, and tank pressure $P_{tank} = 20\ MPa$ was assumed for simulation purpose [57].

3.10 Electrical Load Consumption Model

We created a hourly base load consumption model for one year [58]. We deemed 50 Symmetrical house electrical load-demand and Some common load for $24h$.

The load curve from the **Table 3.3** was shown in **Fig. 3.3.a**.

Load Demand Uncertainty: We used a MATLAB built-in function called Gaussian Process Regression Models in order to crate variance in the Load-demand. So yearly load demand curve had his different amplitude throughout the year. [59]

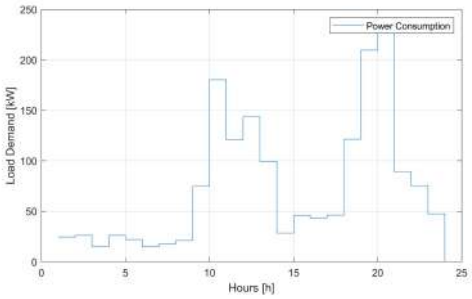

Fig. 3.3.a Hourly Load Demand (Day 1)

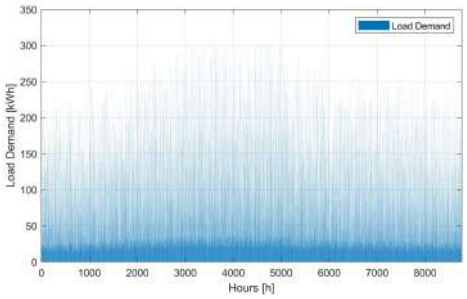

Fig. 3.3.b Annual Load Demand

Fig. 3.3 Hourly Load Consumption

Table 3.3 Residential Load

Sl. No.	Type	Quantity	Power	Hr/day	Wh/day
1	Lights	10	30	8	2,400
2	Fans	3	70	9	1,890
3	Computer, Laptop, TV, mobile-phones etc.		350	7	2,450
4	Electrical-Stove, Refrigerators, Washing-machine etc.		500	10	5,000
5	Air-conditioner	1	1000	5	5,000
6	Other Utilities		100	5	500
	Total Electrical Energy Consumption for 1 House				17.21 kW h/Day
	Total Electrical Energy Consumption for 50 House				860.5 kW h/Day
	Other Utility Services Lift, pump etc.)				100 kW h/Day
	Total Load demand				960.5 kW h/Day

3.11 Energy Dispatch Strategy

We proposed an algorithm for smartly dispatching energy whose operation was shown in **Fig. 3.4**. The Main purpose of the algorithm was to distribute energy generated from Renewable resources to energy storage and load demand more efficiently. This proposed algorithm linked every component of micro gird - PV panel, Wind turbine, Battery Storage, Electrolyzer, Fuel Cell, and hydrogen storage with load-consumption model and Conventional Grid. At first, We estimated renewable energy production from primary generator - Solar PV model and wind turbine model based on their respective Solar irradiation data, Wind speed velocity data. Then total hourly Generated energy was compared with hourly load demand. Based on this comparison, the algorithm split into two route. When hourly generation was greater than hourly load demand then program went through Re-

serve state. The program then check if battery SOC was less than or equal to 80%. If the battery SOC was under 80%, Battery would start charging. When battery SOC was above 80%, then the battery charging was stop. Excess energy then would forwarded to the H_2 Tank Checker Condition. This condition would check if the H_2 tank was under its max capacity. If the hydrogen tank was empty, Then the excess energy would went to the Electrolyzer and converted excess energy into H_2 gas. After that, gas was compressed and stored into H_2 tank with help of compressor. If H_2 tank was full, then the hourly excess energy was sold to CG at 50% of retails electricity cost, the price data was given on **Table 3.5**. EM route had another if-condition checker named EE. EE checked two condition — if the H_2 tank was full and if excess energy was exceeding installed EM capacity. If any of this two condition was true then the hourly excess energy was sold to CG at 50% of retails electricity cost. As for second route which was named deficit state, When the hourly load-demand was greater than hourly renewable generation. The algorithm would first checked if the battery SOC was under 20% or not, When the SOC was above 20%, Battery would stated to discharging. When the Battery SOC falls under 20%, in order to satisfied the demanded energy, program then checked if the H_2 tank was empty or not. If the tank was empty, then the shortage power was purchased from CG at retail price. FC route had another if-condition checker named SE. SE checked two condition — if the H_2 tank was low or empty and if shortage energy was exceeding installed FC capacity. If any of this two condition was true then the hourly shortage energy was purchased from CG at retails electricity cost.The price data was given on **Table 3.5**. If no Electrolyzer module was used, then excess power would directly sold to CG after battery was its max SOC, and similarly if Fuel cell was used then shortage power would directly bought from CG when battery SOC was at is min SOC.

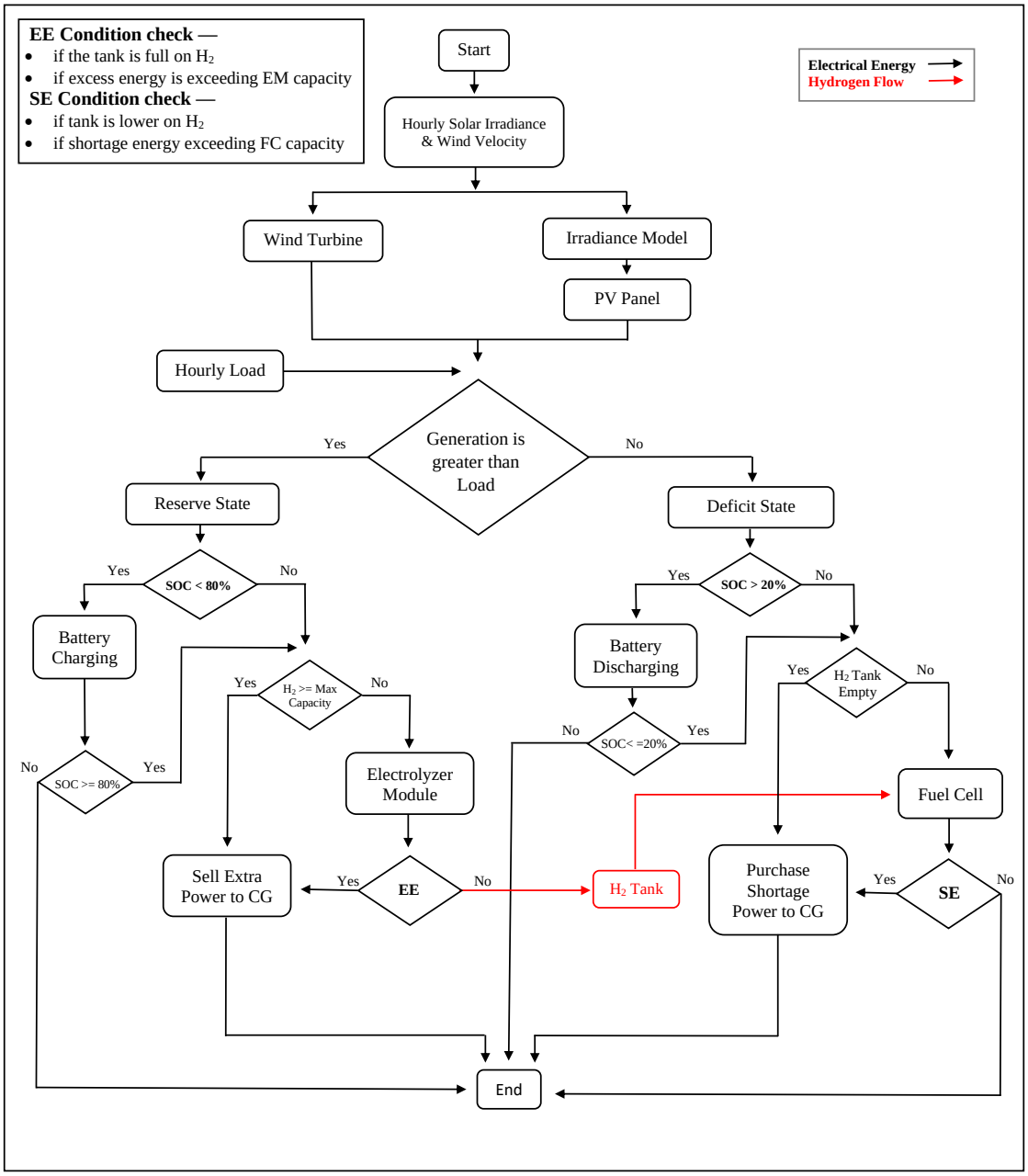

Fig. 3.4 Energy Dispatch Strategy

3.12 Optimization Objective function

Main objective of the microgird sizing was to find out optimal number of component needed for economically feasible operation. Optimal number of component would make up minimum upfront cost as well as minimum cost of energy. We established the (3.24) to minimize the size of our microgrid.

$$F(O) = min \sum_{n=1}^{n_{max}} \left(Component_{quantity} \times Component_{Price} \right) \tag{3.24}$$

Here, n is the number of component for microgrid which was needed to be optimized. $Component_{quantity}$ = PV, WT, BAT, EM, FC, H_2 TANK, and the $component_{price}$ was the capital cost for each component is given on **Table 3.6**

3.12.1 Penalty Function

We used (3.12.1) on our optimization algorithms for solving constrained optimization problems.

$$Penalty = 0, \quad if \quad \sum_{t=1}^{8760} \left(P_{generation} - P_{consumption} \right) > 0$$

$$Penalty = 10^{10}, \quad if \quad \sum_{t=1}^{8760} \left(P_{generation} - P_{consumption} \right) < 0$$

$$F(O) = F(O) + Penalty$$

3.12.2 Constraints

- Number of component is a integer, where $n = 0$ and $n_{max} = [1000, 1000, 500, 500, 500, 100]$ for PV, WT, BAT, EM, FC, H_2 Tank.

$$n \leq Component_{quantity} \leq n_{max}$$

- Lead acid battery was operational if battery SOC stays between 20% to 80%.

$$20\% \leq SOC(t) \leq 80\% \tag{3.25}$$

- H_2 cylinder model was operational if cylinder pressure lied between 27 bar to 135 bar

$$27\ bar \leq Pressure(t) \leq 135\ bar$$

- If the annual total generation doesn't match the annual total load consumption. Then penalty function are triggered, was shown in 3.12.1.

- We tested different microgrid energy penetration levels in terms of peak power distribution capabilities to load demand respective to conventional grid. When, Pene-

tration was set to 25%, 50%, 75% and 100%, EDS had the flexibility to take 25%, 50%, 75% and 100% of total load demand from conventional grid respectively. 100% Penetration means microgrid would try to maintain the full load demand and not bought energy from conventional grid.

3.13 Particle Swarm Optimization Model

We used the particle swarm optimization (PSO) method to minimize the number of component need for microgrid along with lowering the Installation Cost, LCOE and GHG emission, the flowchart of PSO operation was shown in **Fig. 3.5**

3.13.1 PSO Operation

We briefly discussed the procedures involved in the operation of PSO:

3.13.1.1 Initialization

Initially, at time t, we generated random sets n particles using *rand*() function of MATLAB, where $upper\ \ limit = 1000$ was the maximum number of component can be installed, and the $lower\ \ limit = 0$ was for every components. The population, $pop(t) = [X_1(t), X_2(t), ...X_n(t)]^T$. Swarm population was the population of moving particles that tend to cluster together while each particle seems to be moving in a random direction.

3.13.1.2 Individual Best

In PSO operation, As the particle moved across the search space, it compares its present fitness value to the best fitness value it had ever had at any point since the process began. We evaluated the individual best using $X_j^*(t) = [X_{j,1}^*(t), X_{j,2}^*(t), ..., X_{j,m}^*(t)]$

3.13.1.3 Global Best

We used the following equation- $J(X^{**}(t)) \leq J(X_j^*(t)), j = 1, 2, ..., n$ to evalute the global best among all the individual best.

3.13.1.4 Weight Updating

(3.26) was applied to update the inertia weight.

$$w(t) = \alpha w(t-1) \tag{3.26}$$

3.13.1.5 Velocity Updating

(3.13.1.5) was applied to update velocity of swarm population using the individual best and the global best J^{th} velocity of particle in the k^{th} dimension update respectively.

$$\mathrm{v}_{j,k}(t) = w(t)v_{j,k}(t-1) + c_1 r_1(x^{*}_{j,k}(t-1) - x_{j,k}(t-1)) + c_2 r_2(x^{**}_{j,k}(t-1) - x_{j,k}(t-1)) \quad (3.27)$$

3.13.1.6 Position Updating

(3.28) was used to update position based on velocities of particle.

$$x_{j,k}(t) = v\,j,k(t) + x\,j,k(t-1) \quad (3.28)$$

3.13.1.7 Termination Criteria

We used this termination criteria, if within 500 *iteration* there was no significant improve in new solution, then it was triggered.

3.13.1.8 PSO Flowchart

We used the algorithm shown in **Fig. 3.5**. First we generated random swarms of particle population using random function of MATLAB. This particle must had been integer according to the first constraints of PSO optimization. Then we evaluated each swarm of population with our objective function. If any of the constraints didn't full fill, the algorithm was programmed to add a big penalty with the optimal value. By doing so, the PSO did minimize the objective function value along with the fact it won't come to such value of MG configuration that cannot satisfy the load demand for given MG-CG energy penetration scenario. By doing so we can generation the best particle among first swarm of population. The personal best score and global best score was saved in different variable. After that program went through second iteration. This time the program will update the weight and velocity of the particle and also check the boundary that that program didn't exceed the minimum or the maximum limit of the particle count. Program would've went through the given number of iteration or it meets the termination criteria. In **Table 3.4** the necessary parameter for PSO optimization was given.

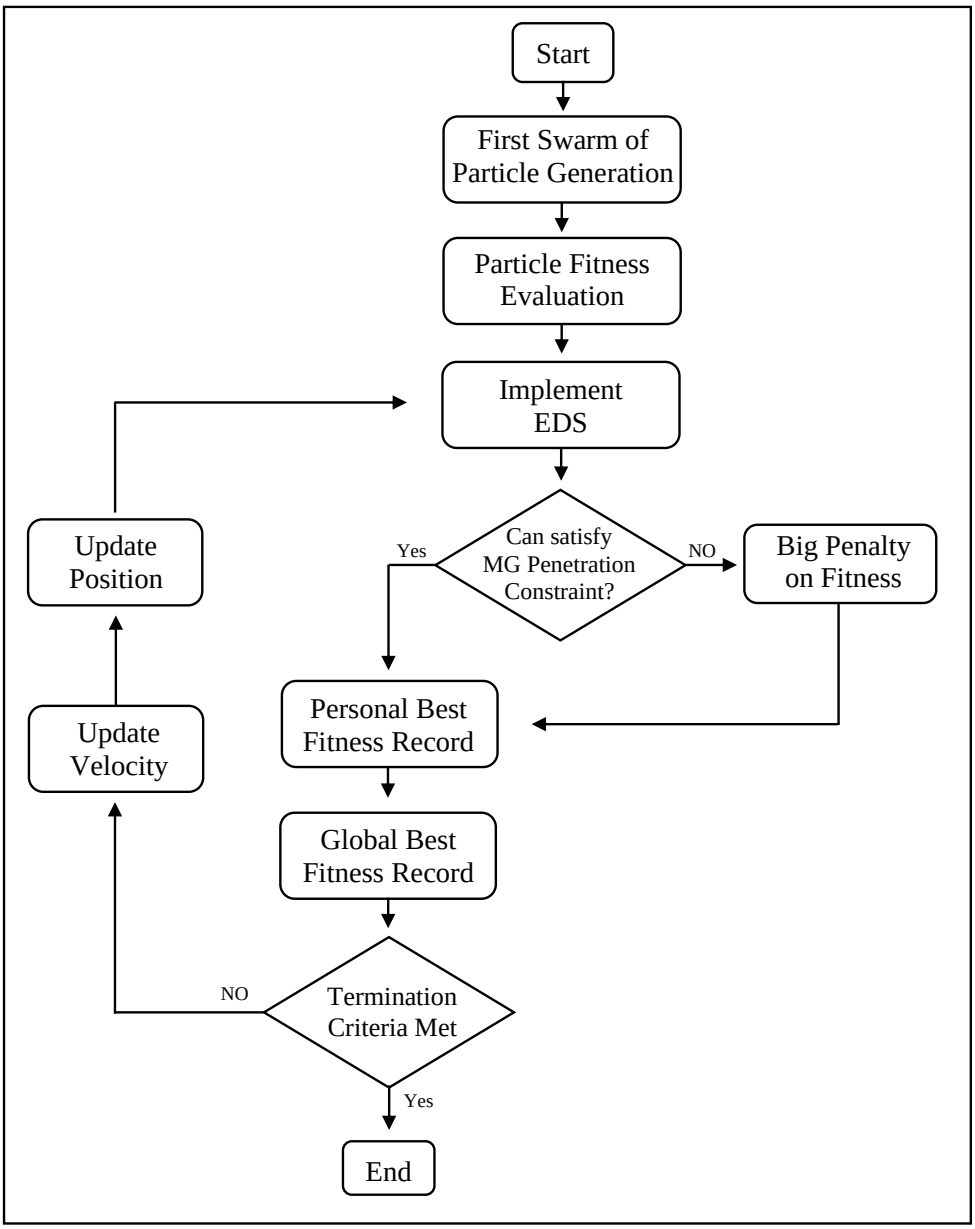

Fig. 3.5 Particle Swarm Optimization Flowchart

Table 3.4 Particle Swarm Optimization Parameter

Parameter	Swarm of Particle	Max Iteration	Termination Criteria	Total Run
Value	100	10000	500	3

3.14 Economic assessment model

LCEO

We calculated Levelized Cost of Energy ($\$/kWh$) of Grid Connected Microgrid using Equation (3.29) [60].

$$LCOE = \frac{CRF \times NPC + CG_{Purchase} - CG_{Sell}}{AED} \tag{3.29}$$

Here, ($CG_{Purchase}$), and (CG_{Sell}) are the yearly summation of total power sold to CG and purchase from CG. Per unit price was given on **Table 3.5**.

$$\begin{aligned} CG_{Sell} &= \sum_{t=1}^{t=8760} (E_{sell} \times Per\ Unit\ Sell\ Price) \\ CG_{Purchase} &= \sum_{t=1}^{t=8760} (E_{purchase} \times Per\ Unit\ Purchase\ Price) \end{aligned} \tag{3.30}$$

CRF

We calculated the CRF using the equation (3.31) [60].

$$CRF = \frac{IR(1+IR)^T}{(1+IR)^T - 1} \tag{3.31}$$

Where, IR is the interest rate, T is the MG lifetime.

NPC

We estimated the NPC using the equation (3.32) [60].

$$\begin{aligned} NPC = PV\ Cost + WT\ Cost + BAT\ Cost + EM\ Cost + \\ FC\ Cost + H_2\ Tank\ Cost + Inverter\ Cost \end{aligned} \tag{3.32}$$

Table 3.5 Spain Per Unit Electricity Prices [61]

Operation	Price ($ /kWh)
Per Unit Energy Buy from CG	0.252
Per Unit Energy Sell to CG	0.111

We calculated all the individual Present value using equation bellow -

$$\begin{aligned} PV\ Cost &= IC_{pv} + MC_{pv} \\ WT\ Cost &= IC_{wt} + MC_{wt} + RC_{wt} \\ BAT\ Cost &= IC_{bat} + RC_{bat} \\ EM\ Cost &= IC_{em} + MC_{em} + RC_{em} \\ FC\ Cost &= IC_{fc} + MC_{fc} + RC_{fc} \\ H_2\ Tank\ Cost &= IC_{H_2\ tank} + MC_{H_2\ tank} \\ Inverter\ Cost &= IC_{inverter} + MC_{inverter} \\ IC_{inverter} &= Rating_{inverter} + K_{Price} \end{aligned} \tag{3.33}$$

We estimated the IC, MC, and RC of each component using the equation (3.34), (3.35), and (3.36) respectively.

Installation Cost (IC)

$$IC_k = (K_{quantity} \times K_{Price}) \tag{3.34}$$

Operation and Maintenance Cost (O&MC)

$$MC_k = K_{quantity} \times K_{Per\ watt\ MC} \times \sum_{n=1}^{N} \left(\frac{1+ER}{1+IR}\right)^T za \tag{3.35}$$

Replacement Cost (RC)

$$RC_k = K_{quantity} \times K_{Per\ watt\ RC} \times \sum_{n=5,10,15}^{N} \left(\frac{1+ER}{1+IR}\right)^T \tag{3.36}$$

Here, $'K'$ was the type of component $i.e-PV,\ WT,\ EM,\ FC,\ BAT,\ H_2\ tank, and\ Inverter$. Number of component used in MG, $K_{quantity}$ was determined using Genetic Algorithm, price of each component, $K_{Price} = K_{capacity}\ (W) \times$ Per watt cost of $'k'$ component $(\$/W)$, $K_{Per\ watt\ MC}$, $K_{Per\ watt\ RC}$, and T was the lifetime of each component, and these data was given on **Table 3.6**.

Table 3.6 Price Table of Microgrids Components [10], [60]

Component Name	Per Unit Capaity	Capital Cost	Operation & Maintenance	Replacement Cost	Lifetime (Years)
PV Panel	0.435 kW	468 ($)	4.35 ($)	-	20
Wind Turbine	1 kW	950 ($)	19 ($)	800 ($)	20
Battery	12kWh (12V, 1000 Ah)	350 ($)	-	300 ($)	10
Inverter	10 kW	100 ($/kW)	-	-	10
Electrolyzer	1 kW	2000 ($)	10 ($/year)	1500 ($)	10
Fuel Cell	1 kW	3000 ($)	60 ($/year)	2500 ($)	15
H2 Tank	6 kg/Per Unit	3960 ($)	79.2 ($/year)	-	20

3.15 Environmental Assessment

Even if actual production of renewable energy have been emission-free, some GHG emissions occur during life cycle stages. This also provides in formation on sources to decrease the GHG and carbon emissions for renewable generator and storage [62], [63]. Here, we estimated the LCA of our model.

3.15.1 Estimation of GHG Emission

We estimated the GHG emissions (*kg CO*2 *equivalent*) on the basis of life cycle assessment (*LCA*) of power generation using the (3.37).

$$Emission_{total} = \sum_{t=1}^{k=6} (AG \times E) \tag{3.37}$$

Here, AG was the annual generation by each component of Microgrid, and E was the emission factor, the data was given on **Table 3.7**.

Table 3.7 Emission Factors [62]

Component Name	LCA GHG emission ($Kg\ CO_2\ eq./kWh$)
PV Panel (mono-silicon)	0.045
Wind Turbine ($v \approx 6.5\ m/s$)	0.01
Lead Acid Battery (per kWh stored)	0.028
Electrolyzer	0.011
Fuel Cell	0.15
Spain CG [64]	0.1660

CHAPTER 4

SIMULATIONS AND RESULTS

4.1 Introduction

In **chapter 3**, we had discussed about the mathematical modeling of each component of the system, applying Energy Dispatched algorithm, and eventually minimize the levelized cost of energy using Genetic algorithm and Particle swarm optimization technique. Lastly we looked over annual GHG emission of the system. We used the software environment of MATLAB R2021a, and the hardware environment of Intel Core i5 CPU, 3.40 GHz, 8 GB memory, and the operating system Windows 11 64-bit for all the calculation. In this chapter we exhibited the final output results of our microgrid model.

4.2 Site selection

We selected the metrological data sets of solar irradiance and wind velocity of Madrid, a city of Spain. Spain was among the first to adopt large-scale solar PV, and it has an excellent potential, area greater than 20000 km^2 which is almost 4% of the country can be utilize for harnessing solar energy [65]. We collected the location specific hourly wind velocity and solar irradiance data from the Data Access Viewer of **NASA POWER** [6].

4.3 Renewable Resource of Madrid

Hourly meteorological data of wind velocity and solar irradiation for Madrid was given on **Fig. 4.1**, **Fig. 4.2.a**, and **Fig. 4.2.b**.

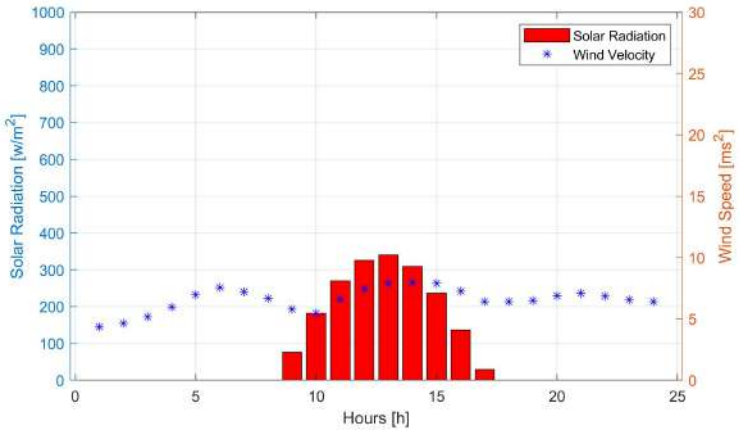

Fig. 4.1 Meteorological Data for Day 1 (Solar and Wind)

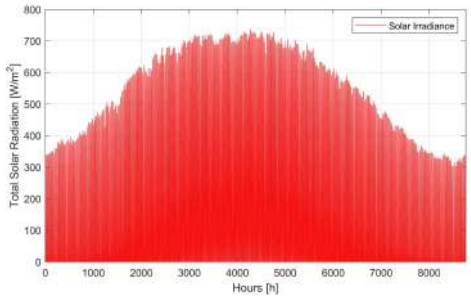

Fig. 4.2.a Hourly Solar Irradiance

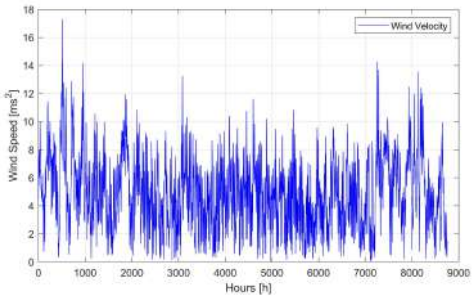

Fig. 4.2.b Hourly Wind Speed

Fig. 4.2 Meteorological Data for Year One

4.4 MG Optimization Output

Optimal Size of Grid-Connected microgird was achieved by PSO algorithm, where we've determined the four optimal configuration MG-CG energy penetration scenario considering economical and environmental impact. The output convergence Curve of PSO for 25%, 50%, 75%, and 100% MG-CG energy penetration levels were given on **Fig. 4.3**.

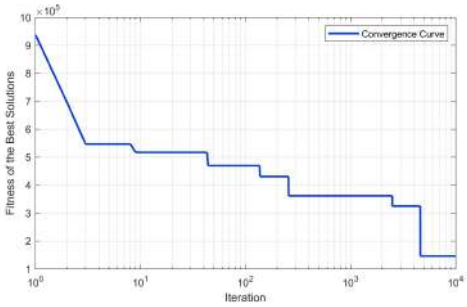

Fig. 4.3.a 25% MG Penetration Level

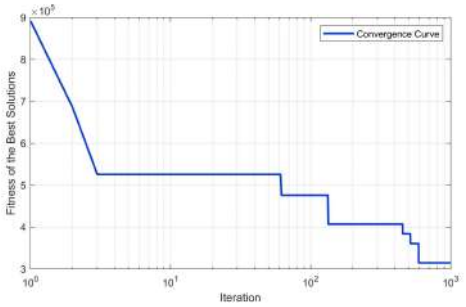

Fig. 4.3.b 50% MG Penetration Level

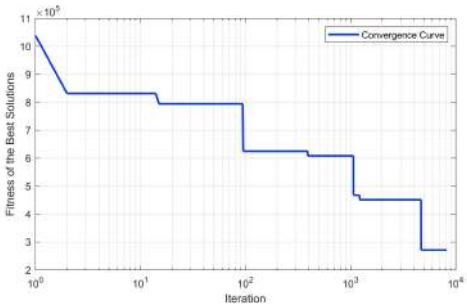

Fig. 4.3.c 75% MG Penetration Level

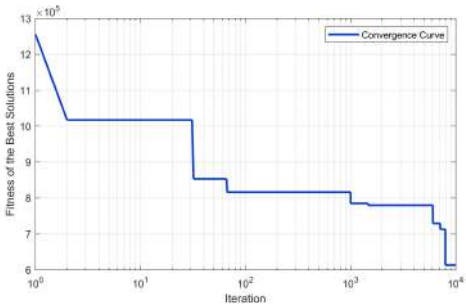

Fig. 4.3.d 100% MG Penetration Level

Fig. 4.3 Optimization Convergence Curve for all MG Penetration levels

4.5 Microgrid EDS Overview

The hourly renewable energy generation by PV and WT was determined using the methodology shown in **Chapter 3**. and the load demand data was generated based on **Table 3.3**. The first 24 hour of renewable generation and load demand for 4 different MG-CG energy

penetration scenarios were shown in **Fig. 4.4**.

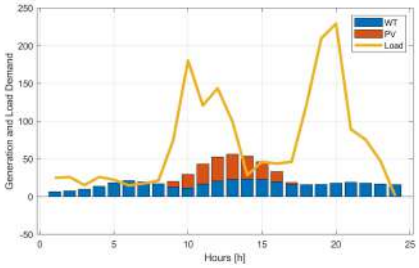

Fig. 4.4.a 25% Penetration

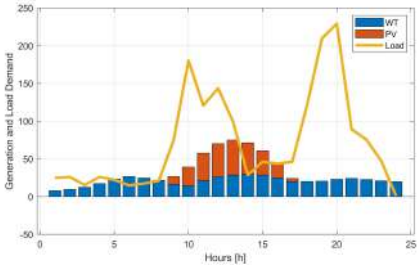

Fig. 4.4.b 50% Penetration

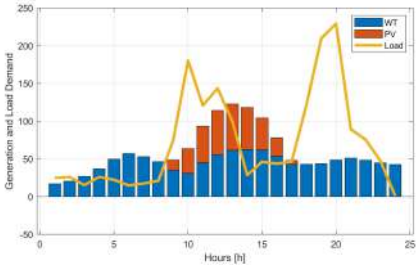

Fig. 4.4.c 75% Penetration

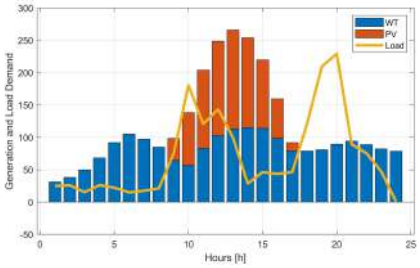

Fig. 4.4.d 100% Penetration

Fig. 4.4 Hourly Generation and Load Demand for all MG penetration levels (Day 1)

Daily total renewable generation and load consumption data of 365 days (1 year) for each 25%, 50%, 75%, and 100% MG-CG penetration scenarios were shown in **Fig. 4.5**.

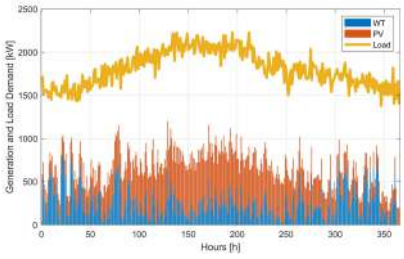

Fig. 4.5.a 25% Penetration

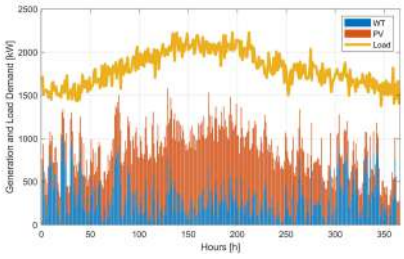

Fig. 4.5.b 50% Penetration

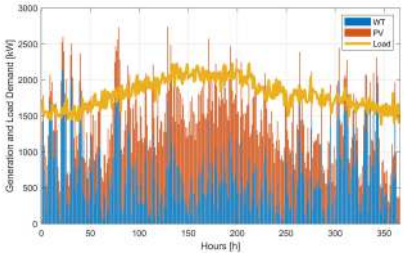

Fig. 4.5.c 75% Penetration

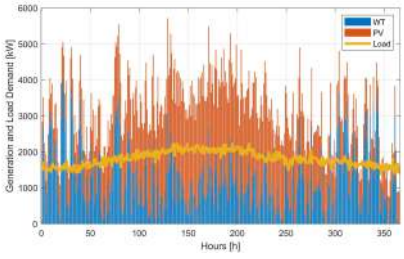

Fig. 4.5.d 100% Penetration

Fig. 4.5 Yearly EDS Overview for different MG penetration levels

First 24 hours of microgrid's Energy Dispatched data was shown in **Fig. 4.6**, where

balance means the difference between renewable generation and load demand. When balance is positive which means, generation is higher and the excess energy will be distributed between Battery and hydrogen storage. When balance is negative that means shortage energy will be deliver from battery, hydrogen system or power grid.

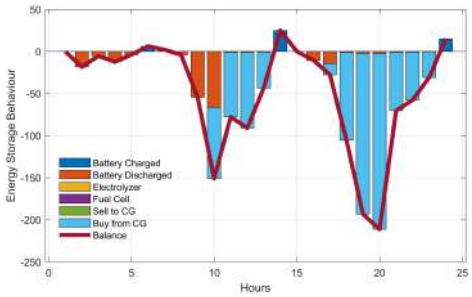

Fig. 4.6.a 25% Penetration

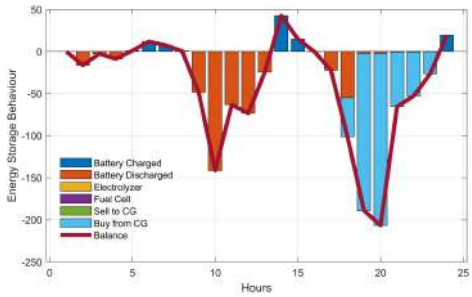

Fig. 4.6.b 50% Penetration

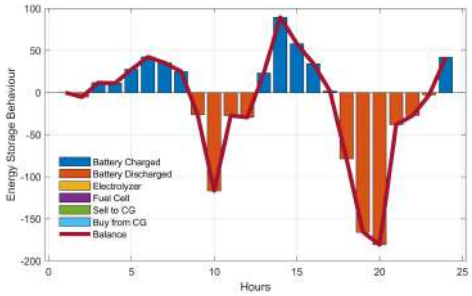

Fig. 4.6.c 75% Penetration

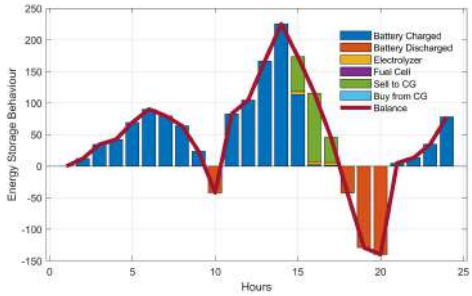

Fig. 4.6.d 100% Penetration

Fig. 4.6 EDS for different MG penetration levels (Day 1)

Monthly microgrid's Energy Dispatched data was shown in **Fig. 4.7**. Here total energy consumption and generation has been displayed using bar plot. We can get a clear idea about which components is used how much through out the year.

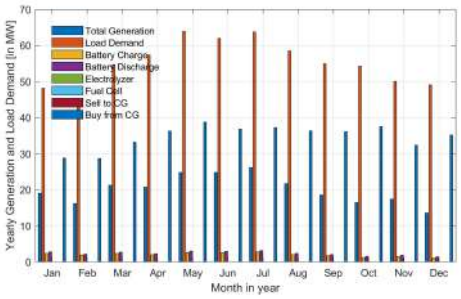

Fig. 4.7.a 25% Penetration

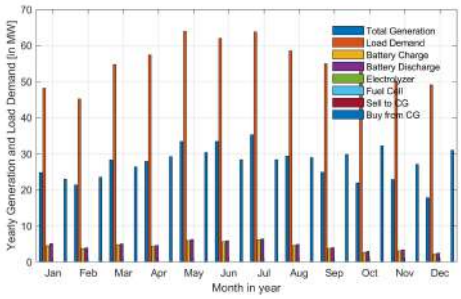

Fig. 4.7.b 50% Penetration

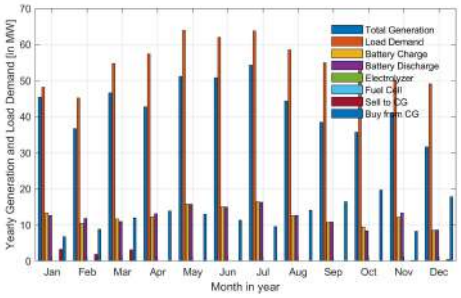

Fig. 4.7.c 75% Penetration

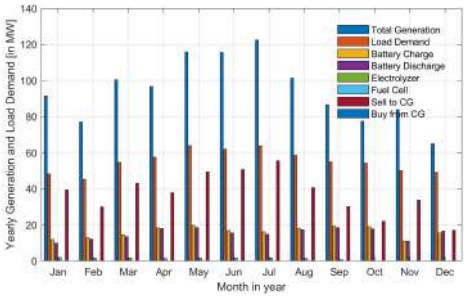

Fig. 4.7.d 100% Penetration

Fig. 4.7 Yearly EDS for different MG penetration levels

4.6 Comparison of all MG configuration

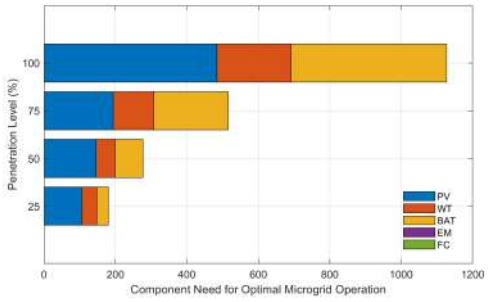

Fig. 4.8.a Components Size

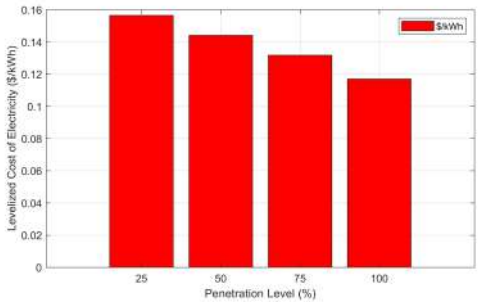

Fig. 4.8.b LCOE

Fig. 4.8 Size and LCOE for all Penetration Levels

Different Components size and LCOE ($\$/kWh$) has found for each 25%, 50%, 75%, and 100% MG-CG penetration scenarios were shown in **Fig. 4.8.a** and **Fig. 4.8.b** respectively. Here, **Table 4.1**, Shows the individual renewable generation and load demand though out the year. The total amount of energy bought and sold to conventional grid annually for four different MG-CG energy penetration level scenario.

In **Table 4.2**, We showed the numbner of MG components needed, Levelized cost of energy, and the upfront cost, and the annual greenhouse gas emission to run the system

Table 4.1 Annual Generation and Consumption of Different MG Penetration Level

Energy Generation and Consumption (MWh/yr)								
Penetration Level	**PV**	**WT**	**Total Generation**	**Load Demand**	**Electrolyzer**	**Fuel Cell**	**Sold to CG**	**Bought from CG**
25%	149.05	90.70	239.76	659.79	0	0	0	415.95
50%	205.30	114.46	319.76	659.79	0	0	0	336.75
75%	272.79	244.05	516.83	659.79	0	0	8.62	150.70
100%	680.57	449.22	1129.77	659.79	0	0	460.05	0

with respective MG-CG energy penetration levels.

Table 4.2 Overall Comparison of Different MG Penetration Level

Microgrid										Conventional Grid	
Penetration Level	PV	WT	BAT	EM	FC	H2 Tank	LCEO ($/kWh)	Investment Cost ($)	GHG (tonne CO2 eq./yr)	CEO	GHG
25%	106	42	32	0	0	0	0.15	100665.6	76.25	0.08	109.87
50%	146	53	78	0	0	0	0.14	145919.6	65.61		
75%	194	113	209	0	0	0	0.13	271214.1	38.86		
100%	484	208	435	5	7	2	0.11	613088.4	32.74		

In **Table 4.3**, We breakdown the overall economic analysis including investment cost, levelized cost, present value cost and every components cost for four different MG-CG energy penetration levels. For each MG-CG energy penetration level, the amount of energy purchase and sold the conventional grid are also been included in the table.

Table 4.3 Economic Overview of Different MG Penetration Level

Name	**Cost ($)**			
Penetration Level	**25%**	**50%**	**75%**	**100%**
Solar PV	50984.65	70224.12	93311.50	232797.76
Wind Turbine	234574.19	296010.28	631116.25	1161700.7
Battery	27443.42	66893.33	179239.81	373058.93
Inverter	2692.03	2692.03	2692.03	2692.02
Electrolyzer	0	0	0	43124.22
Fuel Cell	0	0	0	98957.46
H2 Tank	0	0	0	6373.48
Sold to Grid	0	0	861.93	46004.02
Buy from Grid	83179.08	67349.21	30138.23	0
Investment Cost	100665.6	145919.6	271214	576168.4
Present Value Cost	315694.25	435819.74	906359.57	1770249.41
LCOE	0.1565 ($/kWh)	0.1441 ($/kWh)	0.1317 ($/kWh)	0.1008 ($/kWh)

4.7 Comparison with similar studies

LCEO for different MG configuration of literature was given on Comparison table has been shown in **Table 4.4**.

Table 4.4 LCEO ($\$/kWh$) Comparison Table of Similar Studies

Sl. No	MG Configurations	Location	LCOE ($/kWh)	Reference
1	PV, WT, BAT, H2 System, Grid	Spain	0.11 — 0.15	This Study
2	PV, WT, LB, BDG, FC, H2 Tank	USA	0.43 — 0.86	[62]
3	PV	USA	0.13 — 0.16	[66]
4	PV, WT, DG	Singapore	0.19 — 0.30	[51]
5	PV, WT, BIOMASS, LB, DG	India	0.25 — 0.27	[67]
6	PV, WT, FC	Iran	0.55 — 0.81	[68]
7	PV,WT, DG	SA	0.34	[69]

CHAPTER 5
CONCLUSION

5.1 Introduction

This is the endmost chapter that deduces our thesis work. We have attempted to provide a comprehensive summary of the work starting from looking over the fundamental concepts, system design, methodology, simulations data. Afterwards We have given assessment considering economical and environmental impact of our work. Limitations and potential future scope of this thesis have also been discussed.

5.2 Conclusion

In this thesis work, We have implemented the hybrid energy storage system in grid connected scenario, where we have done a comparative study of a grid-connected microgrid system with 25%, 50%, 75% and 100% energy penetration levels. We showed how MG's annual output, economical cost, environmental impact would vary depending on various MG penetration levels. Sizing of MG was done by PSO, so that we could achieve the optimal MG configuration. Optimal amount of MG component would drastically cut-down the installation cost as well as levelized cost of electricity. After testing different energy penetration scenario we found the LCOE lies between $0.11 $0.15. Best LCOE was achieved when the MG penetration level was 100%. But as for Installation cost, the minimum result was achieved when the penetration cost was minimum. The annual Greenhouse Gas emission was found lowest on MG 100% energy penetration level scenario, where the primary generator source was the RES, so it left fewer carbon footprint considering LCA of DG's.

5.3 Applications of this work

As the fossil energy have been rapidly depleting and the greenhouse gas emission quickly rising, the worlds have been a long search for alternative renewable energy sources and green energy storage. This research study examined how different microgrid configurations and different energy storage system affect LCOE and LCA. Depending on need one could analyse the economical ft of choosing energy storage. And could have clear overview of the system.

5.4 Limitation

Primary objective was to find a optimal configuration for microgrid using optimization technique which is more economically feasible. This studies shows only a approximate feasibility of the microgrid using given circumstances. As the worlds weather is unstable and ever changing, the compensation for uncertainty, intermittency and instability is to resort the smart grid age which have a superior energy storage capability, But still there is no method developed to predict the outcome accurately. Furthermore, aside from energy generation and consumption, there can be numerous fault within the microgrid system, which may hamper the basic operation of microgrid. These are the model's limitations since they are not taken into account.

5.5 Future Work

In this thesis, we proposed a model and estimated the annual generation and cost. But in practical or simulation scenario various factor are existed which acts add many more constraint to the model. Moreover, we have not include BIOMASS in a primary generation unit. The potential of biomass energy is excellent, but it comes with cost. Most electricity generated from biomass is produced by direct combustion. Biomass is burned in a boiler to produce high-pressure steam. BIOMASS can be added to the microgrid system and the yearly GHG emission, LCA and LCOE of microgrid system can be assessed for future scope of work.

REFERENCES

[1] T. Blaschke, M. Biberacher, S. Gadocha, and I. Schardinger, "'energy landscapes': Meeting energy demands and human aspirations," *biomass and bioenergy*, vol. 55, pp. 3–16, 2013.

[2] K. O. Yoro and M. O. Daramola, "Co2 emission sources, greenhouse gases, and the global warming effect," in *Advances in carbon capture*. Elsevier, 2020, pp. 3–28.

[3] M. A. Mirzaei, M. Nazari-Heris, B. Mohammadi-Ivatloo, K. Zare, M. Marzband, and A. Anvari-Moghaddam, "A novel hybrid framework for co-optimization of power and natural gas networks integrated with emerging technologies," *IEEE Systems Journal*, vol. 14, no. 3, pp. 3598–3608, 2020.

[4] IEA, "International energy agency." [Online]. Available: https://www.iea.org/

[5] T. Blaschke, M. Biberacher, S. Gadocha, and I. Schardinger, "'Energy landscapes': Meeting energy demands and human aspirations," *Biomass and Bioenergy*, vol. 55, pp. 3–16, aug 2013.

[6] NASA, "National Aeronautics and Space Administration POWER | Data Access Viewer." [Online]. Available: https://power.larc.nasa.gov/data-access-viewer/

[7] S. I. Seneviratne, M. G. Donat, A. J. Pitman, R. Knutti, and R. L. Wilby, "Allowable co2 emissions based on regional and impact-related climate targets," *Nature*, vol. 529, no. 7587, pp. 477–483, 2016.

[8] EIA, "How much carbon dioxide is produced per kilowatthour of us electricity generation?" 2020.

[9] F. Apadula, C. Cassardo, S. Ferrarese, D. Heltai, and A. Lanza, "Thirty years of atmospheric co2 observations at the plateau rosa station, italy," *Atmosphere*, vol. 10, no. 7, p. 418, 2019.

[10] IRENA, "International renewable energy agency." [Online]. Available: https://www.irena.org/

[11] T. Adefarati and G. Obikoya, "Techno-economic evaluation of a grid-connected microgrid system," *International Journal of Green Energy*, vol. 16, no. 15, pp. 1497–1517, 2019.

[12] M. S. Thopil, R. C. Bansal, L. Zhang, and G. Sharma, "A review of grid connected distributed generation using renewable energy sources in south africa," *Energy strategy reviews*, vol. 21, pp. 88–97, 2018.

[13] A. Colmenar-Santos, S. Campíñez-Romero, C. Pérez-Molina, and M. Castro-Gil, "Profitability analysis of grid-connected photovoltaic facilities for household electricity self-sufficiency," *Energy Policy*, vol. 51, pp. 749–764, 2012.

[14] S. Shivashankar, S. Mekhilef, H. Mokhlis, and M. Karimi, "Mitigating methods of power fluctuation of photovoltaic (pv) sources–a review," *Renewable and Sustainable Energy Reviews*, vol. 59, pp. 1170–1184, 2016.

[15] A. A. Bayod-Rújula, "Future development of the electricity systems with distributed generation," *Energy*, vol. 34, no. 3, pp. 377–383, 2009.

[16] F. Toja-Silva, A. Colmenar-Santos, and M. Castro-Gil, "Urban wind energy exploitation systems: Behaviour under multidirectional flow conditions—opportunities and challenges," *Renewable and Sustainable Energy Reviews*, vol. 24, pp. 364–378, 2013.

[17] J. Jung and M. Villaran, "Optimal planning and design of hybrid renewable energy systems for microgrids," *Renewable and Sustainable Energy Reviews*, vol. 75, pp. 180–191, 2017.

[18] I. Alsaidan, A. Khodaei, and W. Gao, "A comprehensive battery energy storage optimal sizing model for microgrid applications," *IEEE Transactions on Power Systems*, vol. 33, no. 4, pp. 3968–3980, 2017.

[19] T. Ersal, C. Ahn, D. L. Peters, J. W. Whitefoot, A. R. Mechtenberg, I. A. Hiskens, H. Peng, A. G. Stefanopoulou, P. Y. Papalambros, and J. L. Stein, "Coupling between component sizing and regulation capability in microgrids," *IEEE Transactions on Smart Grid*, vol. 4, no. 3, pp. 1576–1585, 2013.

[20] J. Dulout, B. Jammes, C. Alonso, A. Anvari-Moghaddam, A. Luna, and J. M. Guerrero, "Optimal sizing of a lithium battery energy storage system for grid-connected photovoltaic systems," in *2017 ieee second international conference on dc microgrids (icdcm)*. IEEE, 2017, pp. 582–587.

[21] A. A. Moghaddam, A. Seifi, and T. Niknam, "Multi-operation management of a typical micro-grids

using particle swarm optimization: A comparative study," *Renewable and Sustainable Energy Reviews*, vol. 16, no. 2, pp. 1268–1281, 2012.

[22] S. Z. Baykara, "Hydrogen: A brief overview on its sources, production and environmental impact," *International Journal of Hydrogen Energy*, vol. 43, no. 23, pp. 10 605–10 614, 2018.

[23] S. G. Chalk and J. F. Miller, "Key challenges and recent progress in batteries, fuel cells, and hydrogen storage for clean energy systems," *Journal of Power Sources*, vol. 159, no. 1, pp. 73–80, 2006.

[24] L. Meng, E. R. Sanseverino, A. Luna, T. Dragicevic, J. C. Vasquez, and J. M. Guerrero, "Microgrid supervisory controllers and energy management systems: A literature review," *Renewable and Sustainable Energy Reviews*, vol. 60, pp. 1263–1273, 2016.

[25] B. Shyam and P. Kanakasabapathy, "Feasibility of floating solar pv integrated pumped storage system for a grid-connected microgrid under static time of day tariff environment: A case study from india," *Renewable Energy*, 2022.

[26] C. Nayar, M. Tang, and W. Suponthana, "Wind/pv/diesel micro grid system implemented in remote islands in the republic of maldives," in *2008 IEEE international conference on sustainable energy technologies*. IEEE, 2008, pp. 1076–1080.

[27] S. Inamdar, R. Mohanty, P. Chen, R. Majumder, and M. Bongiorno, "On benefits and challenges of nested microgrids," in *2019 IEEE PES Asia-Pacific Power and Energy Engineering Conference (APPEEC)*. IEEE, 2019, pp. 1–6.

[28] P. Sivaraman, C. Sharmeela, P. Sanjeevikumar, C. Sharmeela, and J. B. Holm-Nielsen, "Power system harmonics," *Power Quality in Modern Power Systems*, 2020.

[29] E. Lorenzo, *Solar electricity: engineering of photovoltaic systems*. Earthscan/James & James, 1994.

[30] ucf, "University of central florida." [Online]. Available: https://energyresearch.ucf.edu

[31] A. Dhanola and H. Garg, "Tribological challenges and advancements in wind turbine bearings: A review," *Engineering Failure Analysis*, vol. 118, p. 104885, 2020.

[32] H. W. Langmi, N. Engelbrecht, P. M. Modisha, and D. Bessarabov, "Chapter 13 - hydrogen storage," in *Electrochemical Power Sources: Fundamentals, Systems, and Applications*, T. Smolinka and J. Garche, Eds. Elsevier, 2022, pp. 455–486. [Online]. Available: https://www.sciencedirect.com/science/article/pii/B9780128194249000069

[33] T. Yigit and O. F. Selamet, "Mathematical modeling and dynamic simulink simulation of high-pressure pem electrolyzer system," *International Journal of Hydrogen Energy*, vol. 41, no. 32, pp. 13 901–13 914, 2016.

[34] S. Litster and G. McLean, "Pem fuel cell electrodes," *Journal of power sources*, vol. 130, no. 1-2, pp. 61–76, 2004.

[35] L. Meng, M. Savaghebi, F. Andrade, J. C. Vasquez, J. M. Guerrero, and M. Graells, "Microgrid central controller development and hierarchical control implementation in the intelligent microgrid lab of aalborg university," in *2015 IEEE Applied Power Electronics Conference and Exposition (APEC)*. IEEE, 2015, pp. 2585–2592.

[36] M. L. Darby, M. Nikolaou, J. Jones, and D. Nicholson, "Rto: An overview and assessment of current practice," *Journal of Process control*, vol. 21, no. 6, pp. 874–884, 2011.

[37] L. He, Z. Wei, H. Yan, K.-Y. Xv, M.-y. Zhao, and S. Cheng, "A day-ahead scheduling optimization model of multi-microgrid considering interactive power control," in *2019 4th International Conference on Intelligent Green Building and Smart Grid (IGBSG)*. IEEE, 2019, pp. 666–669.

[38] F. Shahnia, M. Moghbel, A. Arefi, G. Shafiullah, M. Anda, and A. Vahidnia, "Levelized cost of energy and cash flow for a hybrid solar-wind-diesel microgrid on rottnest island," in *2017 Australasian Universities Power Engineering Conference (AUPEC)*. IEEE, 2017, pp. 1–6.

[39] J. Kennedy, "The particle swarm: social adaptation of knowledge," in *Proceedings of 1997 IEEE International Conference on Evolutionary Computation (ICEC'97)*. IEEE, 1997, pp. 303–308.

[40] P. J. Angeline, "Evolutionary optimization versus particle swarm optimization: Philosophy and performance differences," in *International Conference on Evolutionary Programming*. Springer, 1998, pp. 601–610.

[41] Y. Shi and R. C. Eberhart, "Parameter selection in particle swarm optimization," in *International conference on evolutionary programming*. Springer, 1998, pp. 591–600.

[42] M. Iqbal, *An introduction to solar radiation*. Elsevier, 2012.

[43] T. M. Klucher, "Evaluation of models to predict insolation on tilted surfaces," *Solar energy*, vol. 23, no. 2, pp. 111–114, 1979.

[44] A. De Miguel, J. Bilbao, R. Aguiar, H. Kambezidis, and E. Negro, "Diffuse solar irradiation model evaluation in the north mediterranean belt area," *Solar energy*, vol. 70, no. 2, pp. 143–153, 2001.

[45] J. Phang, D. Chan, and J. Phillips, "Accurate analytical method for the extraction of solar cell model parameters," *Electronics Letters*, vol. 20, no. 10, pp. 406–408, 1984.

[46] O. Wasynezuk, "Dynamic behavior of a class of photovoltaic power systems," *IEEE transactions on power apparatus and systems*, no. 9, pp. 3031–3037, 1983.

[47] J. Patel and G. Sharma, "Modeling and simulation of solar photovoltaic module using matlab/simulink," *International Journal of Research in Engineering and Technology*, vol. 2, no. 3, pp. 225–228, 2013.

[48] "Pv data sheet." [Online]. Available: https://us.sunpower.com/sites/default/files/media-library/data-sheets/sunpower-e-series-commercial-solar-panels-e20-435-com-datasheet-521912-revb_1.pdf

[49] "Revista técnica bilingüe de energía," Jun 2022. [Online]. Available: https://futurenergyweb.es/

[50] M. Javidsharifi, H. Pourroshanfekr, T. Kerekes, D. Sera, S. Spataru, and J. M. Guerrero, "Optimum sizing of photovoltaic and energy storage systems for powering green base stations in cellular networks," *Energies*, vol. 14, no. 7, p. 1895, 2021.

[51] C.-H. Li, X.-J. Zhu, G.-Y. Cao, S. Sui, and M.-R. Hu, "Dynamic modeling and sizing optimization of stand-alone photovoltaic power systems using hybrid energy storage technology," *Renewable energy*, vol. 34, no. 3, pp. 815–826, 2009.

[52] J. Divisek, B. Steffen, and H. Schmitz, "Theoretical analysis and evaluation of the operating data of a bipolar water electrolyser," *International journal of hydrogen energy*, vol. 19, no. 7, pp. 579–586, 1994.

[53] J. Larminie, A. Dicks, and M. S. McDonald, *Fuel cell systems explained*. J. Wiley Chichester, UK, 2003, vol. 2.

[54] B. Yodwong, D. Guilbert, M. Phattanasak, W. Kaewmanee, M. Hinaje, and G. Vitale, "Faraday's efficiency modeling of a proton exchange membrane electrolyzer based on experimental data," *Energies*, vol. 13, no. 18, p. 4792, 2020.

[55] R. F. Mann, J. C. Amphlett, M. A. Hooper, H. M. Jensen, B. A. Peppley, and P. R. Roberge, "Development and application of a generalised steady-state electrochemical model for a pem fuel cell," *Journal of power sources*, vol. 86, no. 1-2, pp. 173–180, 2000.

[56] D. Nelson, M. Nehrir, and C. Wang, "Unit sizing and cost analysis of stand-alone hybrid wind/pv/fuel cell power generation systems," *Renewable energy*, vol. 31, no. 10, pp. 1641–1656, 2006.

[57] Ø. Ulleberg, "Stand-alone power systems for the future: optimal design, operation and control of solar-hydrogen energy systems," 1998.

[58] C. Phurailatpam, B. S. Rajpurohit, and L. Wang, "Planning and optimization of autonomous dc microgrids for rural and urban applications in india," *Renewable and Sustainable Energy Reviews*, vol. 82, pp. 194–204, 2018.

[59] Y. Ge, C. Zhou, and D. M. Hepburn, "Domestic electricity load modelling by multiple gaussian functions," *Energy and Buildings*, vol. 126, pp. 455–462, 2016.

[60] M. Gharibi and A. Askarzadeh, "Size and power exchange optimization of a grid-connected diesel generator-photovoltaic-fuel cell hybrid energy system considering reliability, cost and renewability," *International Journal of Hydrogen Energy*, vol. 44, no. 47, pp. 25 428–25 441, 2019.

[61] "Spain electricity prices, september 2021." [Online]. Available: https://www.globalpetrolprices.com/Spain/electricity_prices/

[62] P. Nagapurkar and J. D. Smith, "Techno-economic optimization and social costs assessment of microgrid-conventional grid integration using genetic algorithm and artificial neural networks: A case study for two us cities," *Journal of Cleaner Production*, vol. 229, pp. 552–569, 2019.

[63] I. Kumar, W. E. Tyner, and K. C. Sinha, "Input–output life cycle environmental assessment of greenhouse gas emissions from utility scale wind energy in the united states," *Energy Policy*, vol. 89, pp. 294–301, 2016.

[64] I. Tiseo and F. 16, "Spain: Power sector carbon intensity 2000-2021," Feb 2022. [Online]. Available: https://www.statista.com/statistics/1290486/carbon-intensity-power-sector-spain/

[65] R. Prăvălie, C. Patriche, and G. Bandoc, "Spatial assessment of solar energy potential at global scale. a geographical approach," *Journal of Cleaner Production*, vol. 209, pp. 692–721, 2019.

[66] R. F. D.F, "U.s. solar photovoltaic system cost benchmark: Q1 2017 - nrel," 2017. [Online]. Available: https://www.nrel.gov/docs/fy17osti/68925.pdf

[67] Y. Sawle, S. Gupta, and A. K. Bohre, "Optimal sizing of standalone pv/wind/biomass hybrid energy system using ga and pso optimization technique," *Energy Procedia*, vol. 117, pp. 690–698, 2017.

[68] R. Hosseinalizadeh, H. Shakouri, M. S. Amalnick, and P. Taghipour, "Economic sizing of a hybrid (pv–wt–fc) renewable energy system (hres) for stand-alone usages by an optimization-simulation model: Case study of iran," *Renewable and Sustainable Energy Reviews*, vol. 54, pp. 139–150, 2016.

[69] M. Mohammadi, S. Hosseinian, and G. Gharehpetian, "Optimization of hybrid solar energy sources/wind turbine systems integrated to utility grids as microgrid (mg) under pool/bilateral/hybrid electricity market using pso," *Solar energy*, vol. 86, no. 1, pp. 112–125, 2012.

APPENDIX

Listing 6.1 Main File Optimization

```
clc; clear; close all;

%% choosing resource data;
EnergyStorage='Hybrid'; % Battery/Hydrogen/Hybrid
CityName='Madrid'; % Choose - Madrid/Seville/Chittagong
CityResourceData = city_data(CityName);

%% Loading PSO Optimization Parameter
params = optimization_parameter();

PENLVL= [25,50,75,100]; % testing for 4 different
   Penetration level

%% Optimization Start
for i=1:length(PENLVL)

    CityResourceData.PP = PENLVL(i);  % Penetration
       Percentage

    %% Initiating PSO
    OptimizationResults = pso_optimization(params,
       EnergyStorage, CityResourceData);

    fileName = [CityName, '_',EnergyStorage , '_',
       OptimizationResults.OM, '_', num2str(
       CityResourceData.PP)];
    save(fileName);  % Optimization result output save

end

%% 25% Penetration
load('Madrid_Hybrid_PSO_25.mat')
COM25 = OptimizationResults.nComp;
LCA25 = carbon_emissions_estimation(OptimizationResults,
   EnergyStorage, CityResourceData);
MG25 = EDS_Hybrid(OptimizationResults.nComp,
   CityResourceData);
```

```
ECON25 = economic_analysis(OptimizationResults,
   EnergyStorage, MG25);
MG_Output(MG25, ECON25, LCA25, OptimizationResults,
   CityResourceData);

%% 50% Penetration
load('Madrid_Hybrid_PSO_50.mat')
COM50 = OptimizationResults.nComp;
LCA50 = carbon_emissions_estimation(OptimizationResults,
   EnergyStorage, CityResourceData);
MG50 = EDS_Hybrid(OptimizationResults.nComp,
   CityResourceData);
ECON50 = economic_analysis(OptimizationResults,
   EnergyStorage, MG50);
MG_Output(MG50, ECON50, LCA50, OptimizationResults,
   CityResourceData);

%% 75% Penetration
load('Madrid_Hybrid_PSO_75.mat')
COM75 = OptimizationResults.nComp;
LCA75 = carbon_emissions_estimation( OptimizationResults,
   EnergyStorage, CityResourceData);
MG75 = EDS_Hybrid(OptimizationResults.nComp,
   CityResourceData);
ECON75 = economic_analysis(OptimizationResults,
   EnergyStorage, MG75);
MG_Output(MG75, ECON75, LCA75, OptimizationResults,
   CityResourceData);
% 100% Penetration
load('Madrid_Hybrid_PSO_100.mat')
COM100 = OptimizationResults.nComp;
LCA100 = carbon_emissions_estimation(OptimizationResults,
   EnergyStorage, CityResourceData);
MG100 = EDS_Hybrid(OptimizationResults.nComp,
   CityResourceData);
ECON100 = economic_analysis(OptimizationResults,
   EnergyStorage, MG100);
MG_Output(MG100, ECON100, LCA100, OptimizationResults,
   CityResourceData);


%% directory and name format
```

```
folderpath = [cd '\', CityResourceData.cityname,'\',
   EnergyStorage,'\',OptimizationResults.OM,'\'];
resulation = 300;
x0=5;
y0=5;
width=500;
height=300;


%% Annual GHG for All Pen level
PenLevel = [100 75 50 25 0];
SCC100 = [LCA100.PV_Total LCA100.WT_Total LCA100.BAT_Total
    LCA100.EM_Total LCA100.FC_Total LCA100.CG_Total 0];
SCC75 = [LCA75.PV_Total LCA75.WT_Total LCA75.BAT_Total
   LCA75.EM_Total LCA75.FC_Total LCA75.CG_Total 0];
SCC50 = [LCA50.PV_Total LCA50.WT_Total LCA50.BAT_Total
   LCA50.EM_Total LCA50.FC_Total LCA50.CG_Total 0];
SCC25 = [LCA25.PV_Total LCA25.WT_Total LCA25.BAT_Total
   LCA25.EM_Total LCA25.FC_Total LCA25.CG_Total 0];
SCC_NO_MG = [0 0 0 0 0 0 LCA25.CG_ONLY_Total];
TOTAL_EMISSION = [SCC100; SCC75; SCC50; SCC25; SCC_NO_MG
   ].*1e-3;


figure30=figure;
set(gcf,'position',[x0,y0,width,height])
barh(PenLevel, TOTAL_EMISSION, 'stacked'); grid on
xlabel('GHG Emission (tonne CO_2 eq. /yr)');
ylabel('Penetration Level (%)')
legend('PV', 'WT', 'BAT', 'EM', 'FC', 'CG (Buy)', 'Without
    MG')
filename = 'GHG_EMISSION_Vs_PENETRATION_LEVEL';
print([folderpath, filename],'-djpeg',['-r' num2str(
   resulation)])

COM_ALL_PEN = [COM100; COM75; COM50; COM25];
figure31=figure;
set(gcf,'position',[x0,y0,width,height])
PenLevel = [100 75 50 25];
barh(PenLevel,COM_ALL_PEN, 'stacked'); grid on
xlabel('Component Need for Optimal Microgrid Operation');
ylabel('Penetration Level (%)')
```

```
93  legend('PV', 'WT', 'BAT', 'EM', 'FC')
94  filename = 'MG_SIZE_Vs_PENETRATION_LEVEL';
95  print([folderpath, filename],'-djpeg',['-r' num2str(
        resulation)])
96
97
98  PenLevel = [100 75 50 25];
99  LCEO_ALL_PEN = [ECON100.LCOE, ECON75.LCOE, ECON50.LCOE,
        ECON25.LCOE];
100 figure32 = figure;
101 set(gcf,'position',[x0,y0,width,height])
102 bar(PenLevel, LCEO_ALL_PEN, 'stacked', 'r'); grid on
103 ylabel('Levelized Cost of Electricity ($/kWh)');
104 xlabel('Penetration Level (%)')
105 legend('$/kWh')
106 filename = 'LCOE_Vs_PENETRATION_LEVEL';
107 print([folderpath, filename],'-djpeg',['-r' num2str(
        resulation)])
108
109
110 filename = 'LCEO_IC_Vs_PENETRATION_LEVEL';
111 print([folderpath, filename],'-djpeg',['-r' num2str(
        resulation)])
112
113
114 NetTotalEmission_ALL_PEN = [LCA100.NetTotalEmission, LCA75
        .NetTotalEmission,LCA50.NetTotalEmission,LCA25.
        NetTotalEmission];
115 COM_ALL_PEN
116 LCEO_ALL_PEN
117
118 % close all
```